Reconstruction of the mid-Devonian HP-HT metamorphic event in the Bohemian Massif (European Variscan belt)

Stephen Collett, Karel Schulmann, Piérig Deiller, Pavla Štípská, Vít Peřestý, Marc Ulrich, Yingde Jiang, Luc de Hoÿm de Marien, Jitka Míková

Geoscience Frontiers 13 (2022) 101374

HOSTED BY

Contents lists available at ScienceDirect

Geoscience Frontiers

journal homepage: www.elsevier.com/locate/gsf

Research Paper

Reconstruction of the mid-Devonian HP-HT metamorphic event in the Bohemian Massif (European Variscan belt)

Stephen Collett [a,*], Karel Schulmann [a,b], Piérig Deiller [a], Pavla Štípská [a,b], Vít Peřestý [c], Marc Ulrich [b], Yingde Jiang [d], Luc de Hoÿm de Marien [a], Jitka Míková [e]

[a] Centre for Lithospheric Research, Czech Geological Survey, Klárov 3, 118 21 Praha 1, Czech Republic
[b] Institut Terre et Environnement de Strasbourg, UMR 7063 Université de Strasbourg — CNRS, 1 Rue Blessig, 67084 Strasbourg, Cedex, France
[c] Institute of Petrology and Structural Geology, Charles University, Albertov 6, Praha 2 128 43, Czech Republic
[d] State Key Laboratory of Isotope Geochemistry, Guangzhou Institute of Geochemistry, Chinese Academy of Sciences, Guangzhou 510640, China
[e] Laboratories of the Czech Geological Survey, Geologická 6, 15200 Praha 5, Czech Republic

ARTICLE INFO

Article history:
Received 20 September 2021
Revised 30 November 2021
Accepted 18 February 2022
Available online 22 February 2022
Handling Editor: R. Palin

Keywords:
Variscan Orogeny
Avalonian-Cadomian Orogeny
Eclogite
Geochemistry
Zircon Lu–Hf geochronology

ABSTRACT

Mid-Devonian high-pressure (HP) and high-temperature (HT) metamorphism represents an enigmatic early phase in the evolution of the Variscan Orogeny. Within the Bohemian Massif this metamorphism is recorded mostly in allochthonous complexes with uncertain relationship to the major tectonic units. In this regard, the Mariánské Lázně Complex (MLC) is unique in its position at the base of its original upper plate (Teplá-Barrandian Zone). The MLC is composed of diverse, but predominantly mafic, magmatic-metamorphic rocks with late Ediacaran to mid-Devonian protolith ages. Mid-Devonian HP eclogite-facies metamorphism was swiftly followed by a HT granulite-facies overprint contemporaneous with the emplacement of magmatic rocks with apparent supra-subduction affinity. New Hf in zircon isotopic measurements combined with a review of whole-rock isotopic and geochemical data reveals that the magmatic protoliths of the MLC, as well as in the upper plate Teplá-Barrandian Zone, developed above a relatively unaltered Neoproterozoic lithospheric mantle. They remained coupled with this lithospheric mantle throughout a geological timeframe that encompasses separate Ediacaran and Cambrian age arc magmatism, protracted early Paleozoic rifting, and the earliest phases of the Variscan Orogeny. These results are presented in the context of reconstructing the original architecture of the Variscan terranes up to and including the mid-Devonian HP-HT event.

1. Introduction

Reconstruction of pre-orogenic architecture is a complex and often difficult process; especially if the orogen of interest involves multiple contrasting terranes or oceanic basins. Isotopic fingerprinting provides a powerful tool in determining the nature and origin of basement rocks within an orogenic belt. Traditionally, this has involved collection of whole-rock isotopic data using the Rb–Sr, Sm–Nd, U–Pb and to a lesser extent the Lu–Hf and Re–Os decay systems (e.g., Nance and Murphy, 1994; Linnemann and Romer, 2002; Ackerman et al., 2020). Instrumental advances in spatially resolved isotopic measurements have additionally enabled the development of mineral isotopic fingerprinting (Thirlwall and Walder, 1995; Blichert-Toft et al., 1997); and many studies of high-grade orogenic belts now routinely incorporate in-situ Lu–Hf isotopic measurements from zircon (e.g., Arenas et al., 2014; Henderson et al., 2016; Tabaud et al., 2021). Zircon is of particular interest as it is a highly resistant mineral capable of retaining its original isotopic signature through multiple erosional-depositional or metamorphic events. Moreover, by targeting the same mass for both U–Pb and Lu–Hf analysis, it is possible to directly link zircon crystallisation ages to the composition of the source (Spencer et al., 2020).

The European Variscan Belt is one of the most well studied orogenic belts on Earth. It developed in response to late Paleozoic convergence between the Laurussia and Gondwana continents during closure of the Rheic Ocean and amalgamation of the Pangea supercontinent (see reviews by Nance et al., 2010, 2012). However, despite the large corpus of research undertaken in the Variscan Belt; controversy persists regarding the original number and distribution of individual terranes and oceanic basins (e.g., Kroner and

* Corresponding author.
E-mail address: stephen.collett@geology.cz (S. Collett).

https://doi.org/10.1016/j.gsf.2022.101374
1674-9871/

Romer, 2013; Stampfli et al., 2013; Franke et al., 2017; Edel et al., 2018). Nevertheless, recent progress has been made towards developing a single unified coherent model for the evolution of the Variscan Belt by utilising large databases of lithological, structural, geochemical, geochronological, and petrological data (e.g., Lardeaux et al., 2014; Casas and Murphy, 2018; Stephan et al., 2019a,b; Martínez Catalán et al., 2020, 2021). A key component of these studies was to identify similarities in the origin and evolution of high-pressure (HP) belts which can be correlated across the entire Variscan Orogen.

For the Bohemian Massif, the easternmost massif of the European Variscan Belt (Fig. 1a), three phases of HP metamorphism can be identified. The earliest phase occurs in the mid-Devonian (*c.* 400 – 380 Ma) reaching eclogite-facies conditions before a pervasive granulite-facies overprint (e.g., O'Brien, 1997; Kryza and Fanning, 2007; Collett et al., 2018; Jastrzębski et al., 2021). A second phase is characterised by blueschist- to eclogite-facies metamorphism in the Late Devonian and Early Carboniferous (*c.* 360 – 350 Ma) (e.g., Schmädicke et al., 1995, 2018; Konopásek et al., 2019; Collett et al., 2020), while the third phase is associated with spectacular occurrences of Carboniferous (*c.* 355 – 335 Ma) ultra-HP and ultra-high-temperature assemblages (e.g., Medaris et al., 1995, 2006; Kotková, 2007; Kotková et al., 2011; Ackerman et al., 2016; Maierová et al., 2021; Závada et al., 2021). Although most models for the development of the Bohemian Massif tend to agree on oceanic passing to continental subduction, either of a vast Ordovician-Carboniferous Saxothuringian Ocean (e.g., Schulmann et al., 2009, 2014; Franke et al., 2017) or of the Rheic Ocean *sensu stricto* (Kroner and Romer, 2013), neither model is particularly satisfying for the mid-Devonian HP-HT phase, which is hardly compatible with pure oceanic subduction-exhumation (e.g., Yamato et al., 2007; Agard et al., 2009). Recent works

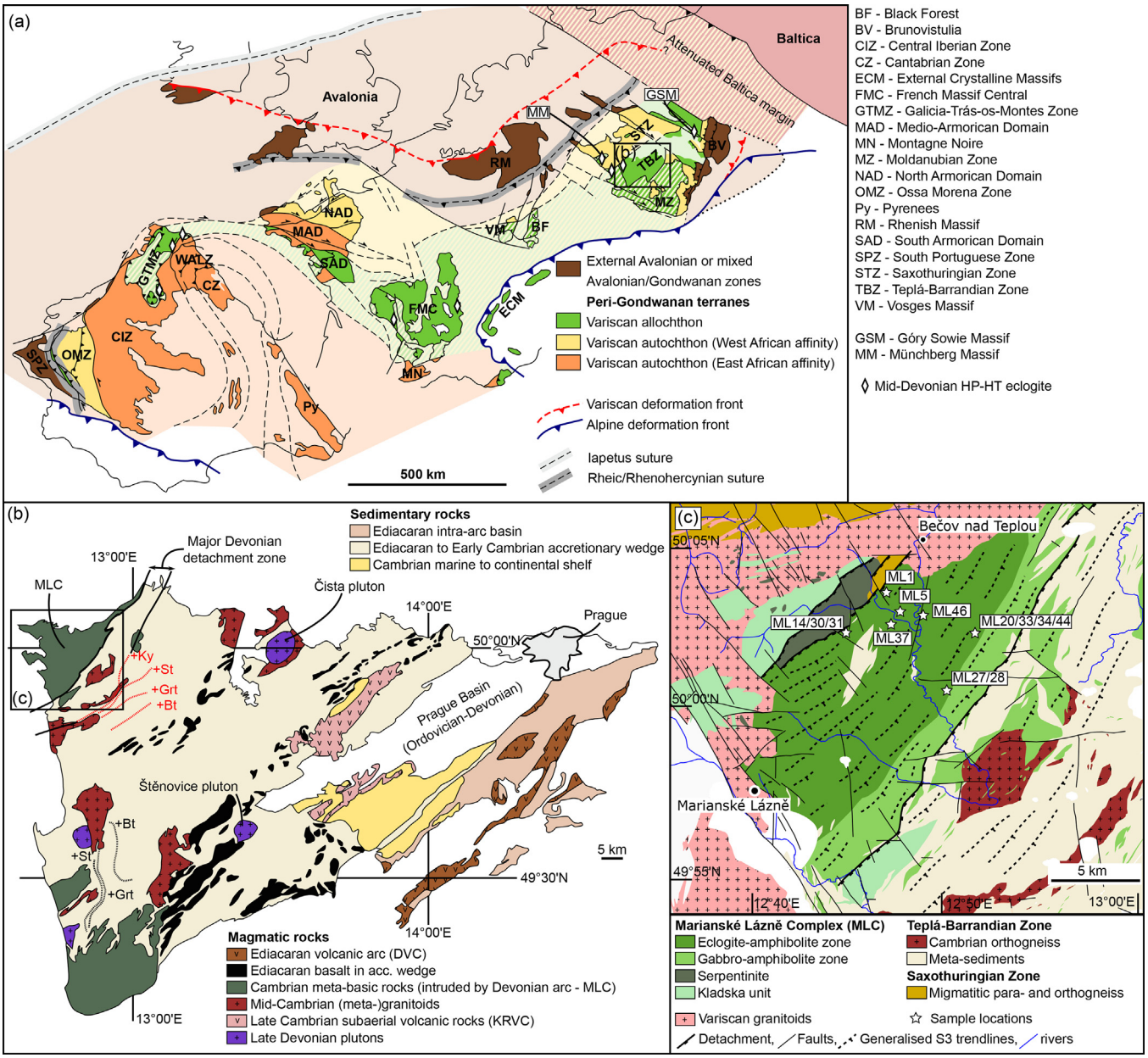

Fig. 1. (a) Tectonic map of the European Variscan Belt modified from Collett et al. (2021); the Variscan allochthon follows definition presented in Martínez Catalán et al. (2020); the Variscan autochthon is split into West African and East African affinity following scheme of Stephan et al. (2019a). (b) Geological map of Teplá-Barrandian Zone modified from Hajná et al. (2018) and Ackerman et al. (2019). (c) Geological map of the MLC and surrounding areas after Collett et al. (2018).

(e.g., Martínez Catalán et al., 2020, 2021) have sought to bridge this gap by drawing comparison with the Galicia-Trás-os-Montes Zone in NW Iberia, where a similar mid-Devonian HP-HT event is well preserved and explained by the subduction of a heterogeneous peri-Gondwanan basin beneath a Cambrian volcanic arc (e.g., Díez Fernández et al., 2020). In this contribution, we test the validity of these correlations through the use of a geochemical, chronological, petrological database supported by new Lu–Hf (and U–Pb) data for zircons from a mid-Devonian HP-HT complex in the NW of the Bohemian Massif. Our presented model from the Late Neoproterozoic to the End Devonian maintains logical consistency with that proposed by Martínez Catalán et al. (2020, 2021) while reconciling some of the key differences observed in the NW Iberian and Bohemian sectors of the Variscan Belt.

1.1. Regional geology

The Bohemian Massif is composed of four principal elements; these are from north to south the Saxothuringian, Teplá-Barrandian, and Moldanubian Zones, each of which is underthrust by Brunovistulia in the east (Fig. 1a). Brunovistulia preserves a long-lasting Neoproterozoic volcanic arc, firstly established on oceanic and latterly continental crust (e.g., Hanžl et al., 2019), and has unclear pre-Variscan relationship to the other parts of the Bohemian Massif (see discussion in Collett et al., 2021). Teplá-Barrandia preserves a complete sequence through a juvenile Neoproterozoic arc and Neoproterozoic to Early Cambrian accretionary wedge (Fig. 1b) overlain by Paleozoic continental to marine basins prior to Mid-Devonian inversion and deposition of flysch-like siliciclastic sediments at the beginning of the Variscan Orogeny (Drost et al., 2004, 2011; Hajná et al., 2018). Saxothuringia is interpreted as a Cadomian retro-arc basin, which became partially molten following termination of subduction in the earliest Cambrian and is overlain by a near complete sequence of Paleozoic shallow continental shelf sediments from the middle Cambrian to the lower Carboniferous (Linnemann et al., 2000, 2004; Linnemann and Romer, 2002). Moldanubia is more enigmatic owing to pervasive high-grade metamorphism, but has been interpreted as a Paleozoic back-arc basin developed on continental crust (e.g., Schulmann et al., 2009, 2014; Pertoldová et al., 2010).

Within the Bohemian Massif, the Devonian-Carboniferous Variscan Orogeny is characterized by two distinct stages; an initial (*c.* 400–380 Ma) stage involved the imbrication of high-pressure nappes with intra-oceanic arc assemblages (ages and P–T conditions of which are summarised in Martínez Catalán et al. (2020, 2021)). And a later (*c.* 365–335 Ma) collisional stage is characterized by the development of granulite-migmatite domes which enclose boudins of ultra-HP and ultra-HT mantle fragments (e.g., Schulmann et al., 2009, 2014; Ackerman et al., 2020). The latter event has been conceptually linked to the relamination of subducted Saxothuringian continental lithosphere beneath the upper plate of the Teplá-Barrandian and Moldanubian zones (e.g., Schulmann et al., 2009, 2014; Lexa et al., 2011; Maierová et al., 2021); although alternative models invoking multiple continental (Kroner and Romer, 2013) or oceanic (e.g., Faryad et al., 2013; Franke et al., 2017) subduction zones also exist.

Only fragmentary evidence of the earlier Mid-Devonian stage is recorded in the allochthonous Münchberg, Wildenfels, and Frankenburg klippes above Saxothuringia; the zone of Erbendorf-Vohenstrauß above the Saxothuringia-Moldanubia boundary; the Góry Sowie Massif located above Saxothuringian basement and bounded by Devonian ophiolites; and in the Mariánské Lázně Complex at the base of Teplá-Barrandia. Of these complexes, the Mariánské Lázně Complex (MLC) represents the most promising site for unravelling the nature of the Mid-Devonian stage as it is the only segment that remains in structural continuum with its original upper plate.

1.2. Local geology

Based on the pioneering works of Kastl and Tonika (1984) and Jelínek et al. (1997), Collett et al. (2018) and Peřestý et al. (2020) identified three distinct structural-lithological zones within the MLC, a large serpentinite body crops-out at the base of the complex, above which occur the eclogite-amphibolite and gabbro-amphibolite zones (Fig. 1c). Although extensively serpentinized, a predominantly harzburgite protolith of the serpentinite is assumed by local preservation of forsterite + enstatite ± diopside + dissemi nated spinel assemblages (Medaris et al., 2011). Replacement of spinel by chlorite and diopside by tremolite are taken to indicate medium temperature metamorphism prior to serpentinization. Tremolite-actinolite and chlorite-talc schist are abundant at contact between serpentinite and the overlying eclogite-amphibolite zone. The eclogite-amphibolite zone is dominated by migmatitic amphibolite containing boudins of often strongly retrogressed eclogite as well as minor HP granulites and felsic orthogneiss (Fig. 2a). In addition, Deiller et al. (2021) identified rocks preserving magmatic nature that appear to intrude the eclogite-bearing metamorphic edifice (Fig. 2b). These rocks are ranging from gabbroic to more leucocratic compositions and have Mid-Devonian emplacement ages, which post-date eclogite-facies metamorphism. Collett et al. (2018) determined peak pressure conditions for the eclogite-facies event of *c.* 26 kbar, 650 – 750 °C, and an approximate age of 390 Ma was determined on the basis of Lu–Hf garnet geochronology. A range of older (up to 410 Ma) and younger (to 370 Ma) ages had previously been determined by Sm–Nd garnet geochronology (Beard et al., 1995) but may have been modified during thermal overprint. The eclogite-facies assemblages were overprinted by granulite-facies (*c.* 14 kbar, up to 850 °C) and amphibolite-facies assemblages. The granulite-facies overprint occurred around 380 Ma (U–Pb dating on zircon) and cooling ages of 375 – 360 Ma (K–Ar and Ar–Ar mica and hornblende; U–Pb monazite, titanite, and rutile) constrain the amphibolite-facies event (Timmermann et al., 2004, and references therein). The granulite-facies event was also recorded in the host migmatitic amphibolites (e.g., Štědrá, 2001), while the amphibolite-facies overprint was observed in all rock types including the magmatic rocks identified by Deiller et al. (2021). The gabbro-amphibolite zone, which occurs structurally above the eclogite-amphibolite zone, is dominated by medium-grade amphibolites containing bodies of meta-gabbro. These meta-gabbros partially preserve their original igneous assemblage, around which coronitic textures have developed in response to amphibolite- to granulite-facies metamorphism (e.g., Jašarová et al., 2016). The protolith of these meta-gabbros are late Cambrian in age (*c.* 500 Ma) and metamorphic overprint is mid-Devonian (*c.* 380 Ma; Timmermann et al., 2006).

The MLC is overprinted by a large-scale detachment zone (e.g., Peřestý et al., 2020), which separates it from the overlying Blovice Accretionary Complex (Teplá Barrandia). The Blovice Accretionary Complex developed in the Neoproterozoic to early Cambrian and is dominated by greywacke and contains minor basaltic bodies, cherts, and olistostromes interpreted as part of an Ocean Plate Stratigraphy (Ackerman et al., 2019; Hajná et al., 2019). Late Devonian plutons intrude the Blovice Accretionary Complex, including the Čistá pluton (Fig. 1c), which was additionally interpreted by Deiller et al. (2021) as an upper plate equivalent of the Mid-Devonian magmatism in the MLC. The contact between the MLC and the Blovice Accretionary Complex (locally the Teplá Crystalline Complex) is intruded by mid-Cambrian granitoids and was metamorphosed in the Early Ordovician and Late Devonian (Peřestý

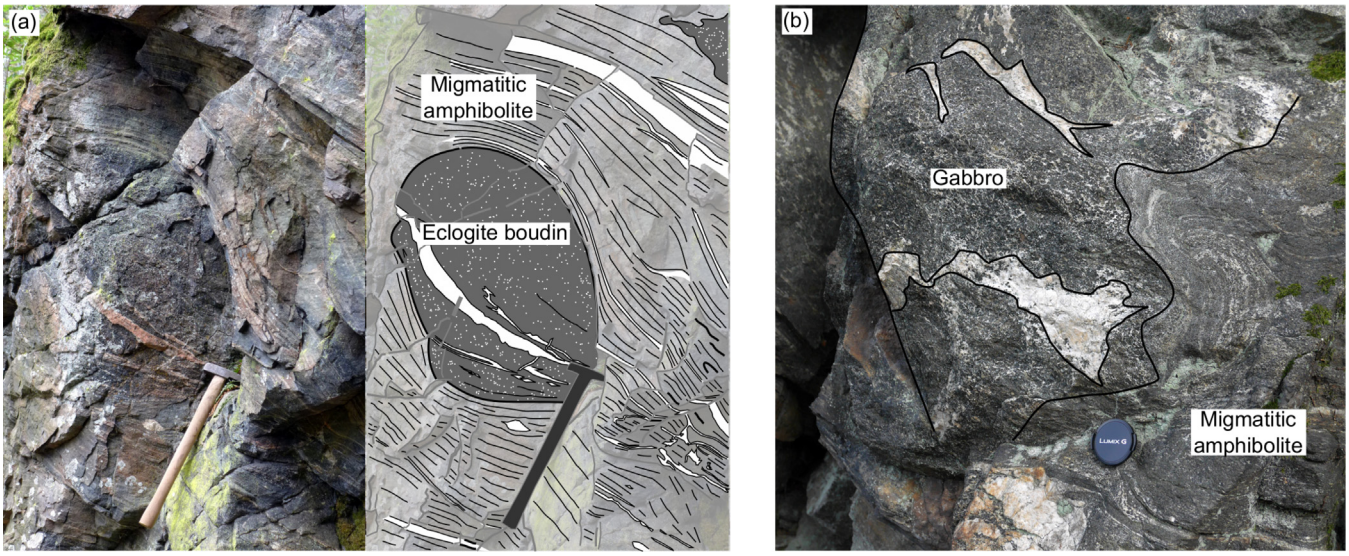

Fig. 2. (a) Field photograph and interpretative sketch of an eclogite boudin in the MLC enclosed in migmatitic amphibolite. (b) Gabbroic rock with felsic segregations intruding migmatitic amphibolite.

et al., 2017). Late Devonian Barrovian-type metamorphism in the Teplá Crystalline Complex shares common geothermal gradient with the granulite-facies event in the MLC (Jašarová et al., 2016; Peřestý et al., 2017; Collett et al., 2018).

Beneath the MLC, low-grade meta-basite and meta-sediments of the Kladská Unit have been inferred to belong to the frontal margin of Saxothuringia (e.g., Kachlík, 1993). This relationship however is obscured by numerous Variscan granitoids of the Karlovy Vary stock which separate the Kladská Unit from Saxothuringia *sensu stricto* (Fig. 1c).

2. Summary of geochemical data

Several studies have published whole-rock geochemical and isotopic data from the MLC; Beard et al. (1995) provided whole-rock major oxide and rare earth element data as well as Sr and Nd isotopic analyses for eclogite, amphibolite, and meta-gabbro; Crowley et al. (2002) conducted a comprehensive geochemical study of 'metabasite', without providing explicit petrological information; Timmermann et al. (2004) studied a whole suite of lithologies from the MLC and provided whole rock major oxide and limited trace element data alongside Sr and Nd isotopic data; Jašarová et al. (2016) studied the meta-gabbro from the gabbro amphibolite zone and overlying Teplá Crystalline Complex conducting total whole-rock analysis of these rocks; and, Deiller et al. (2021) studied the magmatic rocks in the eclogite amphibolite zone, providing complete whole rock analysis alongside Sr and Nd isotopic measurements. Deiller et al. (2021) also included whole-rock analytical data from eclogite as a supplement and Collett et al. (2018) provided Nd–Hf isotopic data from two eclogite samples. A geochemical database is included as a supplement (Supplementary Data A) to this article and additionally includes previously unpublished whole-rock data from the two eclogite samples studied by Collett et al. (2018), whole rock data from the serpentinite body and associated chlorite-talc schist as well as literature data for magmatic rocks from Teplá-Barrandia. The data has been processed using the GCDkit software package (Janoušek et al., 2006a) and summarized in Fig. 3.

Most of the eclogite (Deiller et al., 2021) and metabasites (Crowley et al., 2002) have compositions of typical sub-alkaline basalts; a few metabasites are more SiO_2-rich corresponding to basaltic andesite to andesite compositions (Fig. 3a). The meta-gabbros from the gabbro-amphibolite zone typically have more alkali compositions, characterized by moderately higher Zr/Ti and Nb/Y ratios (Fig. 3a). The Mid-Devonian magmatic rocks of the eclogite-amphibolite zone exhibit a large range from more basic to more acidic compositions in the classification diagrams (Fig. 3a). For the purposes of this article a cut-off of *c.* 60 wt.% of SiO_2 is used to define more basic and more acidic samples within the Devonian magmatic rocks. Notably, some of the more acidic samples have high alkali contents or Zr/Ti ratios plotting in the trachyte and trachy-andesite fields of Fig. 3a. These samples are dominated by oligoclase feldspar and were termed oligoclasite in Deiller et al. (2021).

In the magmatic affinity diagram of Ross and Bédard (2009), the metabasite typically plot more in the tholeiitic field, whereas the eclogites plot more in the transitional field; however, there is once again significant overlap between the two groups (Fig. 3b). The more basic magmatic rocks from the eclogite-amphibolite zone contain both tholeiitic and calc-alkaline members, while the more acidic rocks are almost exclusively calc-alkaline. Primitive mantle normalized (after Sun and McDonough, 1989) spider plots are included as supplementary material (Supplementary Data B), but for ease of presentation several key element ratios are used to present the normalized trace element data in Fig. 3c–g.

The Nb/Nb^* ($Nb_N/(Th_N \times La_N)^{0.5}$) ratio indicate the magnitude of the Nb anomaly with respect to Th and La, the Zr/Zr^* ratio ($Zr_N/(Sm_N \times Nd_N)^{0.5}$) indicates the magnitude of the Zr anomaly with respect to Sm and Nd, La_N/Sm_N indicates fractionation of light rare earth elements (LREE) and Gd_N/Yb_N indicates fractionation of heavy rare earth elements (HREE). Additionally, the Nb/Yb vs Ba/Yb (Fig. 3f) and Nb/U vs Ce/Pb (Fig. 3g) are used to demonstrate relative enrichment or depletion in the large ion lithophile elements (LILE); however, given the high-grade metamorphism of the studied rocks these diagrams can only be interpreted cautiously given the mobility of these elements (Hawkesworth et al., 1993). For eclogite, the Nb/Nb^* ratios are highly variable (0.09 to 3.78); however, a significant cluster of data occurs around 0.5. Similar variability is observed in the Zr/Zr^* ratios (0.19 to 4.69) with a main cluster around 0.7. In general the Nb/Nb^* and Zr/Zr^* ratios are well correlated indicating coupling between the behaviour of the high field strength elements (HFSE). The metabasite show similar

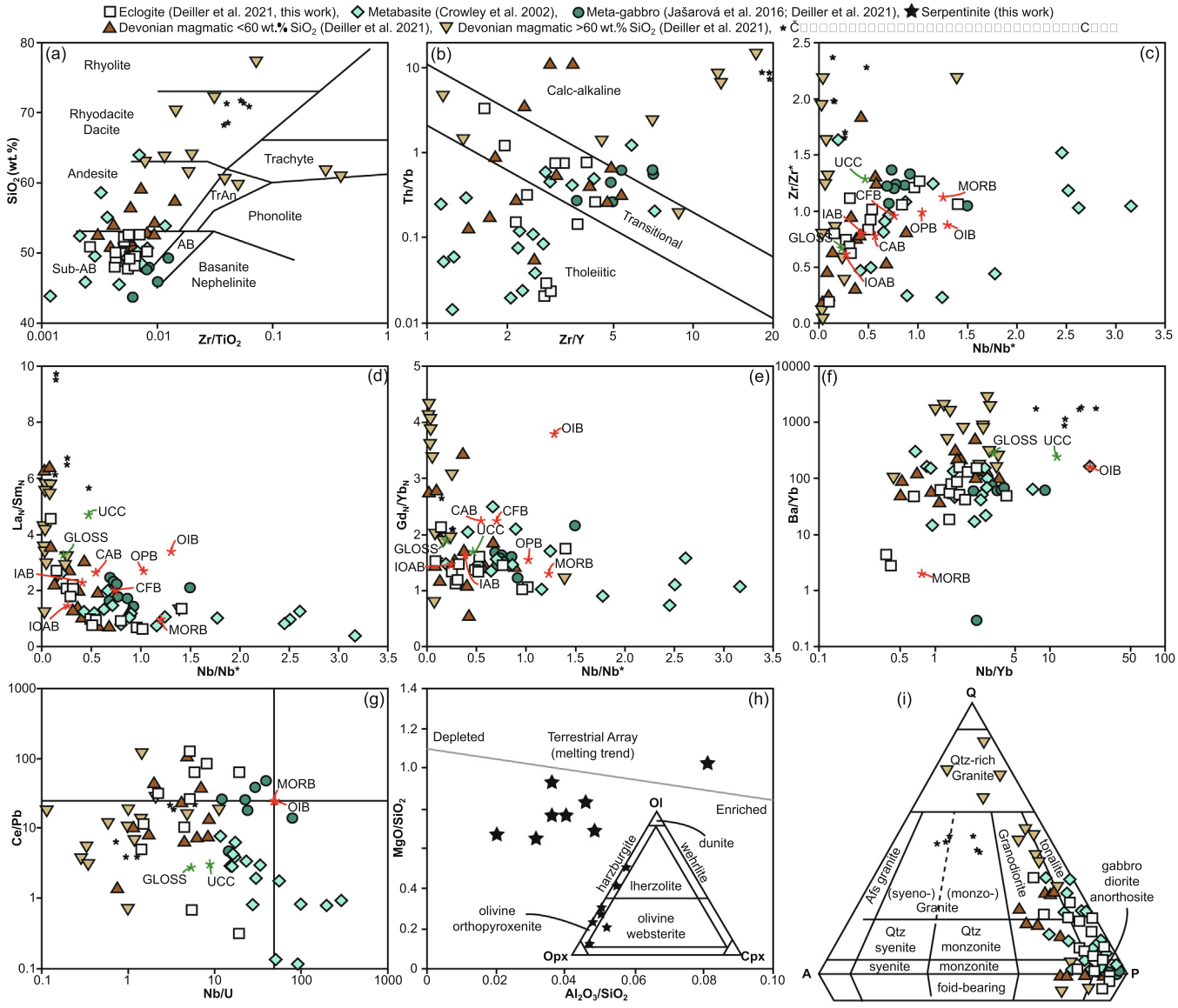

Fig. 3. Whole rock geochemical classification and tectonic discrimination plots. (a) Zr/TiO_2 vs. SiO_2 after Winchester and Floyd (1977); (b) Zr/Y vs. Th/Yb after Ross and Bédard (2009); (c) Nb/Nb* ($Nb_N/(Th_N \times La_N)^{0.5}$) vs. Zr/Zr* ($Zr_N/(Sm_N \times Nd_N)^{0.5}$) plot; (d) Nb/Nb* vs. La_N/Sm_N; (e) Nb/Nb* vs. Gd_N/Yb_N; (f) Nb/Yb vs. Ba/Yb; (g) Nb/U vs. Ce/Pb; (h) Al_2O_3/SiO_2 vs. MgO/SiO_2 for peridotites after Paulick et al. (2006) – inset normative orthopyroxene-olivine-clinopyroxene classification plot; (i) QAPF classification of plutonic rocks (Streckeisen, 1978). All normalisations are to primitive mantle compositions (Sun and McDonough, 1989), reference values for different basaltic settings (red stars) in (c) – (e) after Li et al. (2015), NMORB and OIB compositions in (f) and (g) after Sun and McDonough (1989), upper continental crust (UCC) and global subducting sediments (GLOSS) after Taylor and McLennan (1995) and Plank and Langmuir (1998).

compositional range; however, a significant number of samples (n = 7) exhibit strong (Nb/Nb*>2.5) to extreme (Nb/Nb*>18) Nb enrichment. Although partially correlated, the Zr/Zr* (up to 3.65) do not show such extreme enrichment. Both eclogite and metabasite exhibit low La_N/Sm_N and Gd_N/Yb_N ratios, notably, eclogites with the lowest Nb/Nb* ratio exhibit the highest values for La_N/Sm_N ratio (Fig. 3d). Both the eclogite and metabasite are uniformly enriched in Ba with respect to Nb (Fig. 3f), but exhibit contrasting behaviour in the Nb/U vs Ce/Pb plot (Fig. 3g). The eclogites are uniformly enriched in U with respect to Nb but show variable enrichment or depletion in Pb with respect to Ce, whereas the metabasites are uniformly enriched in Pb but exhibit variable enrichment or depletion in U.

The late Cambrian meta-gabbros show relatively homogeneous compositions, they typically have Nb/Nb* ratios just less than unity and Zr/Zr* ratios slightly above; mean La_N/Sm_N ratios are 1.96 and mean Gd_N/Yb_N ratios are 1.61. One sample is a minor outlier (VP46 – Jašarová et al., 2016), with notably higher Nb/Nb* (1.49) and Gd_N/Yb_N (2.18) ratios. One of the samples is also anomalously depleted in Ba (Fig. 3f), but, otherwise the samples have LILE contents similar to the mantle array (Fig. 3f, g).

The Devonian magmatic rocks are characterised by strong Nb depletion, for the more basic members Nb/Nb* ratios vary from 0.89 down to 0.09, while the more acidic samples, with one exception, exhibit values less than 0.25. In contrast Zr/Zr* ratios are highly variable (0.04 to 4.31), indicating some degree of decoupling between the HFSE. This decoupling is more pronounced for the more acidic samples, but, can also be observed in some of the more basic samples (Fig. 3c). La_N/Sm_N (0.68 to 6.37) and Gd_N/Yb_N (0.54 to 6.60) ratios are also highly variable. For the more basic samples, both ratios are generally lower — although two of the more basic samples (ML31A, ML33C) show the highest La_N/Sm_N ratios — and the two ratios are only weakly correlated. For the more acidic samples there is a strong correlation between the two ratios (i.e., at a

higher La_N/Sm_N ratio the samples exhibit a similarly high Gd_N/Yb_N ratio) with exception of the sample with the highest Gd_N/Yb_N ratio (ML31B), which exhibits a relatively low La_N/Sm_N ratio (1.23). The Devonian magmatic rocks are uniformly enriched in both Ba and U with respect to Nb with greater enrichment in the more acidic samples than the more basic, but exhibit variable enrichment or depletion in Pb with respect to Ce (Fig. 3f, g).

Few high-quality geochemical data points are available from the serpentinite; however, based on their normative mineralogy obtained from the major oxide contents they are consistent with a harzburgite or olivine orthopyroxenite protolith (Fig. 3h). Nonetheless, their Al_2O_3/SiO_2 (0.02 to 0.08) and MgO/SiO_2 (0.66 to 1.03) ratios show some variability and are, with one exception, displaced below the "terrestrial array" of unaltered peridotite (Fig. 3h) defined by Jagoutz et al. (1979). Thorium contents are uniformly below the detection limit (0.1 ppm), precluding calculation of Nb/Nb* ratios. The REE contents of the serpentinite are close to chondritic values and display limited fractionation and no or small Eu anomaly (La_N/Yb_N = 1.27–2.86; Eu/Eu* = 0.74–0.99) with one exception (ML36B) which has high La_N/Yb_N ratio (78.4) and deep Eu anomaly (Eu/Eu* = 0.13).

Also plotted in Fig. 3 are the samples from the Čistá pluton studied by Deiller et al. (2021). Based on their normative mineralogy these are either syeno- or monzo-granites (Fig. 3i). The samples exhibit strong decoupling of the Nb/Nb* (0.14 to 0.48) and Zr/Zr* (1.66 to 2.37) ratios (Fig. 3c) and high La_N/Sm_N ratios (5.65 to 9.71) combined with moderate Gd_N/Yb_N ratios (1.40 to 2.65).

The published whole rock isotopic data are summarised in Fig. 4. The plot of $^{87}Sr/^{86}Sr_{(i)}$ versus $\varepsilon Nd_{(i)}$ (Fig. 4a) indicates that while these are well correlated for amphibolite, some eclogite samples exhibit elevated $^{87}Sr/^{86}Sr_{(i)}$ ratios. These were interpreted by Beard et al. (1995) to be a product of seawater alteration after initial emplacement; however, since both Rb and Sr are highly fluid mobile their ratio may have been altered during fluid-assisted retrogression (e.g., Collett et al., 2021). The Nd isotopic system is more robust to high-grade metamorphism and can reflect original composition of the protoliths of the MLC. Notably, the eclogite and amphibolite show significant heterogeneity; two eclogitic samples show compositions that are even more depleted than the depleted mantle model curve, with $\varepsilon Nd_{(i)}$ values > +10; while another outlier is relatively enriched compared to the depleted mantle reservoir ($\varepsilon Nd_{(i)}$ = − 0.6). The remaining data is spread from + 7.9 to + 5.5 for the eclogite and + 7.9 to + 2.6 for the amphibolite (Fig. 4b). Two data-points from the meta-gabbro show only minor enrichment ($\varepsilon Nd_{(i)}$ = + 6.3 and + 4.9). Most of the Devonian magmatic rocks show similarly minor enrichment with a range of $\varepsilon Nd_{(i)}$ of + 2.2 to + 6.1; two samples (one acidic and one basic) show stronger depletion ($\varepsilon Nd_{(i)}$ = + 8.0) and two acidic samples show more enriched compositions ($\varepsilon Nd_{(i)}$ = + 0.8). Single stage time to depleted mantle model ages (T_{DM}) exhibit a small maxima at 0.65 Ga and main maxima at 1.0 Ga (Fig. 4c), using the more conservative two-stage approach (Liew and Hofmann, 1988) yields a principal maxima around 0.7 Ga with a long shoulder to 1.0 Ga (Fig. 4d). Compiling the data from the MLC against magmatic rocks from Teplá-Barrandia (see Fig. 1b), there is a strong comparability in the isotopic signature with a clear maxima of T_{DM} ages in the mid- to late Neoproterozoic (Fig. 4e).

3. Summary of published and new U–Pb zircon geochronology

Early geochronological work indicated that the protoliths of the MLC must be at least older that the Late Cambrian (*c.* 496 Ma) based on U–Pb zircon dating of a pegmatite (Bowes and Aftalion, 1991) cross-cutting the MLC gabbro. The same authors also published a poorly constrained upper intercept age of 854 ± 130 Ma from a feldspathic gneiss. Timmermann et al. (2004) conducted a more comprehensive zircon (and monazite, rutile, and titanite) U–Pb geochronological study of various different lithologies from the MLC. One eclogite sample, with a strong granulite-facies overprint, yielded a 539 ± 2 Ma crystallisation age, this overlapped within error also with a sample of foliated amphibolite. A second eclogite sample, forming a boudin within the foliated amphibolite, yielded only a single 500 Ma age, which Timmermann et al. (2004) interpreted as inheritance. A high-pressure granulite of intermediate composition also yielded an early Cambrian age, while two samples of meta-gabbro from the gabbro amphibolite zone yielded late Cambrian (*c.* 500 Ma) ages (Timmermann et al., 2006). Timmermann et al. (2004) additionally dated a felsic leucosome from an eclogite boudin that yielded a 378 ± 2 Ma crystallisation age based on dating of titanite. This age overlaps with metamorphic zircon ages from all studied samples as well as monazite dating from an orthogneiss at the base of the eclogite amphibolite zone. More recently, Deiller et al. (2021) presented extensive LA-ICP-MS U–Pb dating of zircon from the magmatic samples from

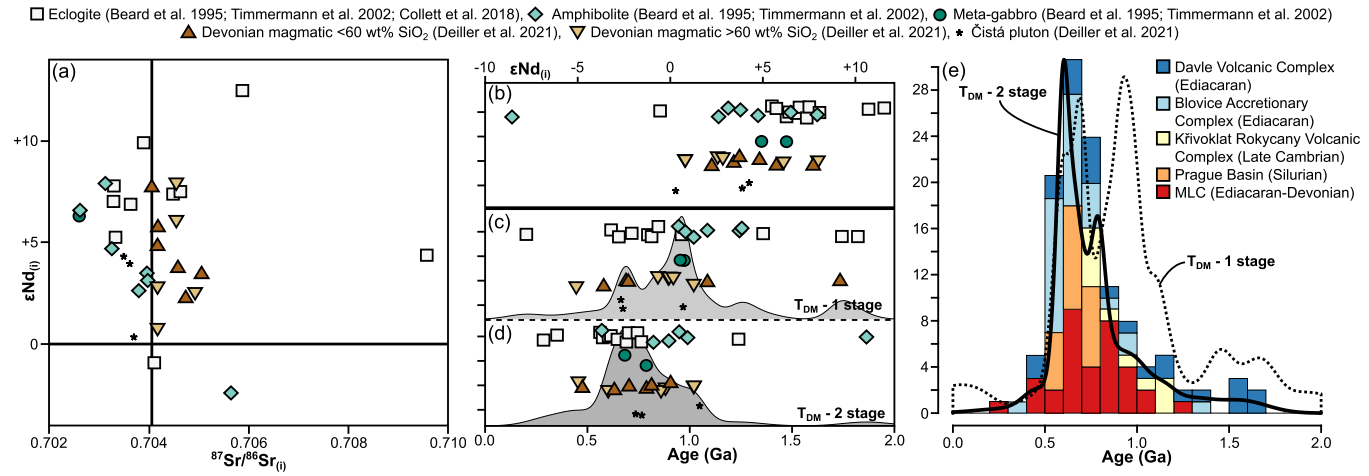

Fig. 4. Plots of whole rock isotopic composition, symbols as in Fig. 3. (a) $^{87}Sr/^{86}Sr_{(i)}$ vs. $\varepsilon Nd_{(i)}$, initial compositions calculated at 525 Ma (eclogite and metabasite), 490 Ma (meta-gabbro), 380 Ma (Devonian magmatic rocks), and 365 Ma (Čistá pluton); (b) strip plot of $\varepsilon Nd_{(i)}$ values in each of the different lithologies of the MLC; (c) strip plot of single-stage time to depleted mantle (T_{DM}) model ages (Ga), grey curve represents a kernel density estimate of the dataset; (d) strip plot of two-stage T_{DM} model ages (Liew and Hofmann, 1988); (e) histogram presenting compilation of two-stage T_{DM} model ages from magmatic rocks from MLC and overlying Teplá-Barrandian Zone. Data from Teplá-Barrandian Zone compiled from: Drost et al. (2004); Pin et al. (2007); Tasáryová et al. (2018); Ackerman et al. (2019); Santolík (2021).

the eclogite-amphibolite zone, their data indicated that these rocks were emplaced in the Mid-Devonian (*c.* 380–390 Ma), broadly contemporaneously with the granulite-facies overprint in the eclogites of the MLC (e.g., Collett et al., 2018). Almost all samples contained inherited cores of early Cambrian and/or Cambro-Ordovician age inferred to have been assimilated from the country rock (i.e., the eclogite and amphibolite of the MLC). In addition, Deiller et al. (2021) published zircon data for two samples of granodiorite from the Čistá pluton, which intrudes the upper plate Blovice Accretionary Complex (Fig. 1b). Their results indicated significant Mid-Devonian inheritance prior to final emplacement at *c.* 365 Ma; these data were taken as evidence that the Čistá Pluton was genetically linked to the Mid-Devonian magmatic rocks of the MLC (Deiller et al., 2021).

We present herein additional LA-ICP-MS U–Pb zircon dating for a sample (ML46-16A) from the eclogite-amphibolite zone. The sample is a retrogressed eclogite containing garnet, surrounded by amphibole-plagioclase kelyphite and a matrix containing diopside-plagioclase-amphibole symplectite after omphacite. The sample has very low Th content (below the 0.1 ppm detection limit) precluding calculation of Nb/Nb* ratio; however, an Nb_N/La_N ratio of 0.74 and Zr/Zr* ratio of 0.78 suggest significant depletion of the HFSE. Zircon occurs both as inclusion in garnet and more commonly within the matrix of the sample; the zircon often have irregular size and shape with longest axis up to 250 μm, and are characterised by contrasting cathodoluminescence dark and light domains (Fig. 5a).

The dating was performed at the Laboratories of the Czech Geological Survey as part of the same session as the data reported in Deiller et al. (2021). The analytical conditions are therefore the same as those reported in Deiller et al. (2021). During the session, all measurements were compared with the GJ-1, Plešovice, and 91500 zircon standards which yielded ages of 610 ± 2 Ma, 338 ± 1 Ma, and 1063 ± 2 Ma, respectively. In total, 82 unknown spot analyses were performed on 54 zircon grains; from which 70 analyses yielded concordant dates (between 95% and 105% concordance). Single grain concordia dates show near continuous spread from 560 Ma to 475 Ma, a single analytical spot yielded a 443 Ma date and five analytical spots from zircon rims yielded dates of 385 Ma to 378 Ma. The five Mid-Devonian dates as well as the single Early Silurian date all exhibit Th/U ratios of less than 0.01, indicating their metamorphic derivation. A multi-grain concordia age of 382 ± 6 Ma (MSWD = 0.32) was calculated for the five Mid-Devonian analyses (Fig. 5a). The Ediacaran-Cambrian dates do not form a coherent population, evidenced by high MSWD (11.9) from a calculated weighted mean (520 ± 4 Ma). Allowing for the fact that some younger dates could be the result of Pb-loss during metamorphism and some older dates may have been inherited from country rock during emplacement a minimum emplacement age of *c.* 495 ± 3 Ma is estimated from a radial plot using the maximum likelihood algorithm of Galbraith and Laslett (1993).

4. Results of Hf in zircon isotopic analysis

Zircons from the sample of retrogressed eclogite (ML46-16A) presented above as well as from the magmatic rocks studied by Deiller et al. (2021) have undergone additional Lu–Hf isotopic measurements. Cathodoluminescence images of representative zircons as well as spot localisations are presented in Fig. 5. The in-situ zircon Lu–Hf isotopic analysis was carried out on a Neptune Plus multi-collector ICP-MS equipped with a Resolution M-50-LR laser-ablation system at the Guangzhou Institute of Geochemistry, Chinese Academy of Sciences. An X skimmer cone in the interface and a small flow of N_2 (2 mL/L) were used to improve the instrumental sensitivity. All masses were collected using Faraday cups employed in a static mode. The laser parameters were set as follows: beam diameter, 40 μm; repetition rate, 6 Hz; energy density, ~4 J cm^{-2}. Helium was chosen as the carrier gas (800 mL min^{-1}).

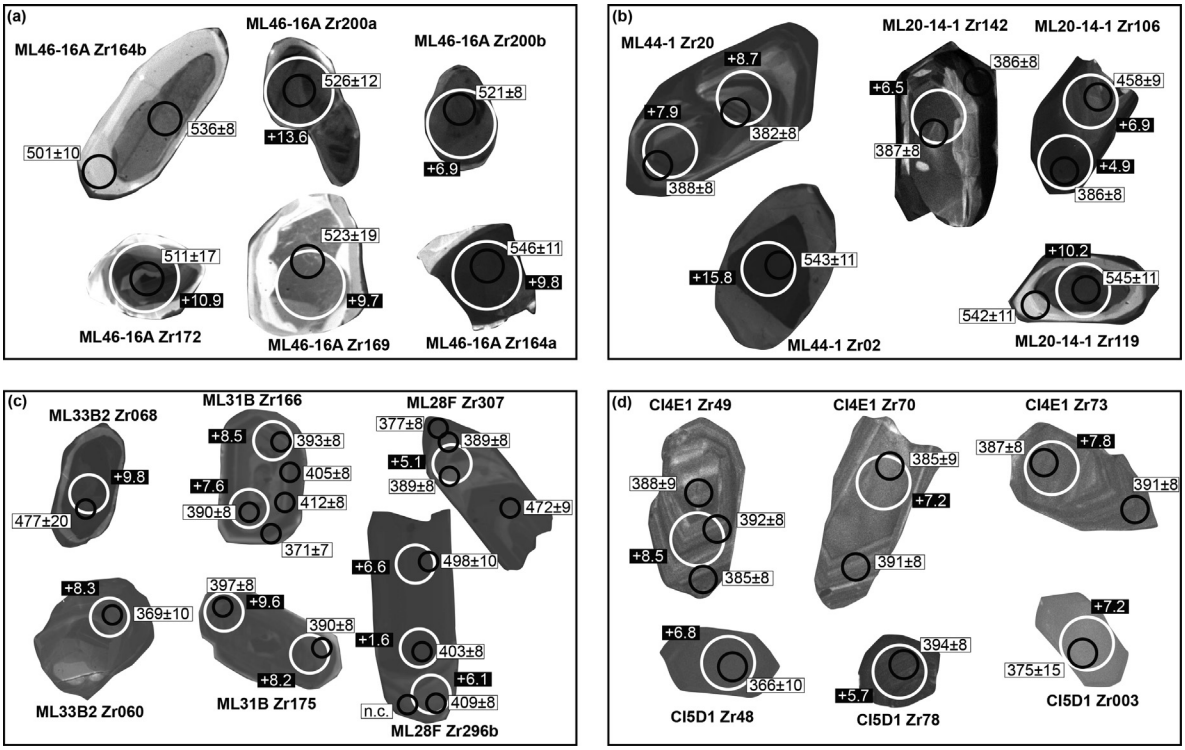

Fig. 5. Representative cathodoluminescence images of zircons from (a) retrogressed eclogite, (b) mafic Devonian magmatic rocks, (c) felsic Devonian magmatic rocks, (d) Čistá Pluton. Black circles represent U–Pb isotopic spots (25 μm diameter) with $^{206}Pb/^{238}U$ date given in white boxes. The white circles represent Lu–Hf isotopic spots (40 μm diameter) with $\varepsilon_{Hf}(t)$ values given in black boxes.

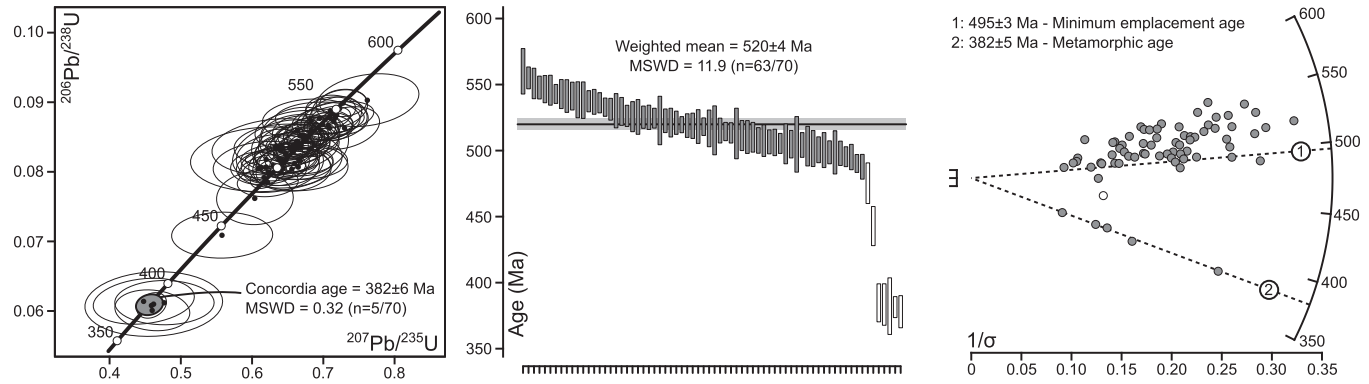

Fig. 6. Results of LA-ICP-MS zircon U–Pb geochronology from eclogite sample ML46-16A plotted using the IsoplotR software of Vermeesch (2018).

Detailed instrumental settings and analytical procedure were reported in Zhang et al. (2014). Forty analyses of the zircon standard Penglai during the course of this study yielded a weighted mean of $^{176}Hf/^{177}Hf = 0.282907 \pm 0.000035$ (2SD), which is consistent within errors with its recommended value in Li et al. (2010).

All Hf-in-zircon isotopic data were calculated with the decay constant of 1.867×10^{-11} yr^{-1} (Söderlund et al., 2004). The chondritic values of $^{176}Hf/^{177}Hf = 0.282772$ and $^{176}Lu/^{177}Hf = 0.0332$ reported by Blichert-Toft and Albarède (1997) were employed for the calculation of $\varepsilon_{Hf}(t)$ values. Complete results are presented in Supplementary Data C and summarised in U–Pb age versus $\varepsilon_{Hf}(t)$ scatter plots in Fig. 7a–d. Two-stage time to depleted mantle model ages (T_{DM}) presented in histograms in Fig. 7e–h and mentioned in the following text were calculated assuming a mean basaltic $^{176}Lu/^{177}Hf$ ratio of 0.022 for the 2nd stage of the model (Lancaster et al., 2011) and the present-day Depleted Mantle values reported by Griffin et al. (2000) and Belousova et al. (2010).

4.1. Retrogressed eclogite

For the sample of eclogite (ML46-16A), Hf isotopic measurements were performed on 11 zircon cores with $^{207}Pb/^{206}Pb$ ages of between 500 Ma and 550 Ma (Fig. 7a). The calculated $\varepsilon_{Hf}(t)$ values range from + 6.9 to + 15.9, both the highest and lowest values are statistical outliers, with the data mostly concentrated between + 8.7 and + 10.9 (n = 8), with a weighted mean of + 10.1 ± 0.3. These data correspond to an average T_{DM} age of 0.72 Ga (Fig. 7e).

4.2. Basic magmatic rocks

Two basic magmatic samples were analysed, ML44-1 and ML20-14–1. Both samples, have Early Cambrian inherited cores and dominant Mid-Devonian age peaks, sample ML20-14-1 additionally contains Early Ordovician age cores (Fig. 7b). Hafnium isotopic measurements targeted both core and rim domains and 24 and 15 analytical spots were measured for sample ML44-1 and ML20-14-1, respectively. The Cambrian cores of sample ML44-1 have highly positive $\varepsilon_{Hf}(t)$ values with a weighted mean of +13.5 ± 0.3 (n = 4). In contrast, the Cambrian cores from ML20-14-1 are only moderately positive ($\varepsilon_{Hf}(t)$ = +9.1 ± 0.5, n = 3), while two analyses on Ordovician cores yielded $\varepsilon_{Hf}(t)$ values of +6.9 ± 2.2 and +11.1 ± 0.8. The $\varepsilon_{Hf}(t)$ values from Devonian cores and rims from sample ML44-1 range between +2.1 and +8.7 (n = 20) with a weighted mean value of +6.5 ± 0.1. Sample ML20-14-1 exhibits similar range of $\varepsilon_{Hf}(t)$ values (+4.9 to +8.1, n = 10) from the Devonian cores and rims with a weighted mean of +7.6 ± 0.2. The calculated T_{DM} model ages for the Cambrian cores of ML44-1 are 0.46 Ga to 0.67 Ga, while the Devonian data yielded T_{DM} model ages of 0.67 Ga to 0.97 Ga with a weighted mean of 0.79 Ga; all of the data from sample ML20-14-1 fall in a calculated T_{DM} range of 0.62 Ga to 0.85 Ga with a weighted mean of 0.75 Ga (Fig. 7f).

4.3. Acidic magmatic rocks

Three acidic magmatic samples were studied from the MLC. These include two tonalitic samples (ML31B and ML33B2), and a sample dominated by oligoclase feldspar (ML28F), which was termed oligoclasite by Deiller et al. (2021). Sample ML31B contained only Mid-Devonian zircon, and 19 zircon Lu–Hf measurements show exclusively positive $\varepsilon_{Hf}(t)$ values (+5.9 to +10.1) with a weighted mean of +8.6 ± 0.2, which corresponds to T_{DM} model ages of 0.61–0.82 Ga with a weighted mean of 0.69 Ga. The second tonalitic sample (ML33B2) contained inherited cores of early Cambrian and Cambro-Ordovician age as well as the main mid-Devonian population (both cores and rims). All three age domains were targeted for Hf isotopic measurements, the early Cambrian cores (n = 3) yielded highly positive $\varepsilon_{Hf}(t)$ values with a weighted mean of +9.3 ± 0.4, the Cambro-Ordovician cores (n = 11) are similarly positive, yielding a weighted mean $\varepsilon_{Hf}(t)$ value of +9.6 ± 0.2. The Devonian grains (n = 16) are mostly concentrated between $\varepsilon_{Hf}(t)$ values of +6.5 to +10.2, besides, an early Devonian outlier, which yielded a less positive value ($\varepsilon_{Hf}(t)$ = +4.8 ± 0.9) and a Mid-Devonian grain, which yielded a negative value and high associated errors ($\varepsilon_{Hf}(t)$ = −6.8 ± 4.4). Excluding the two outliers, yields a weighted mean $\varepsilon_{Hf}(t)$ value of +7.9 ± 0.2. The calculated T_{DM} ages for all domains show strong coherence irrespective of their U–Pb age in the range of 0.59–0.79 Ga, with a weighted mean of 0.71 Ga. The oligoclasite sample (ML28F) contained inherited zircon cores with a mid- to late Cambrian maxima as well as the main Mid-Devonian population. Both age domains were targeted with a combined 9 analytical spots, the $\varepsilon_{Hf}(t)$ values are systematically lower than those of the other felsic samples. The Cambrian cores (n = 5) yielded a weighted mean $\varepsilon_{Hf}(t)$ value of +4.4 ± 0.3, while the Mid-Devonian grains (n = 4) yielded a weighted mean $\varepsilon_{Hf}(t)$ value of + 4.3 ± 0.4. Calculated T_{DM} ages are therefore older, in the range of 0.82 – 1.11 Ga (Fig. 7g).

4.4. Čistá pluton

The samples from the granodioritic Čistá Pluton contained both Mid-Devonian and Late-Devonian zircon, and less commonly, Late-Devonian overgrowths could be observed on euhedral oscillatory zoned Mid-Devonian cores (Deiller et al., 2021). Both the Mid-Devonian and Late Devonian domains were targeted for Hf isotopic measurements from two samples (Cl4E, and Cl5D). Both samples show similarly positive $\varepsilon_{Hf}(t)$ in the range of +5.7 to +10.2. Combining the data from both samples, the Mid-Devonian domains (n = 17) yield a weighted mean $\varepsilon_{Hf}(t)$ value of +7.7 ± 0.2, and the

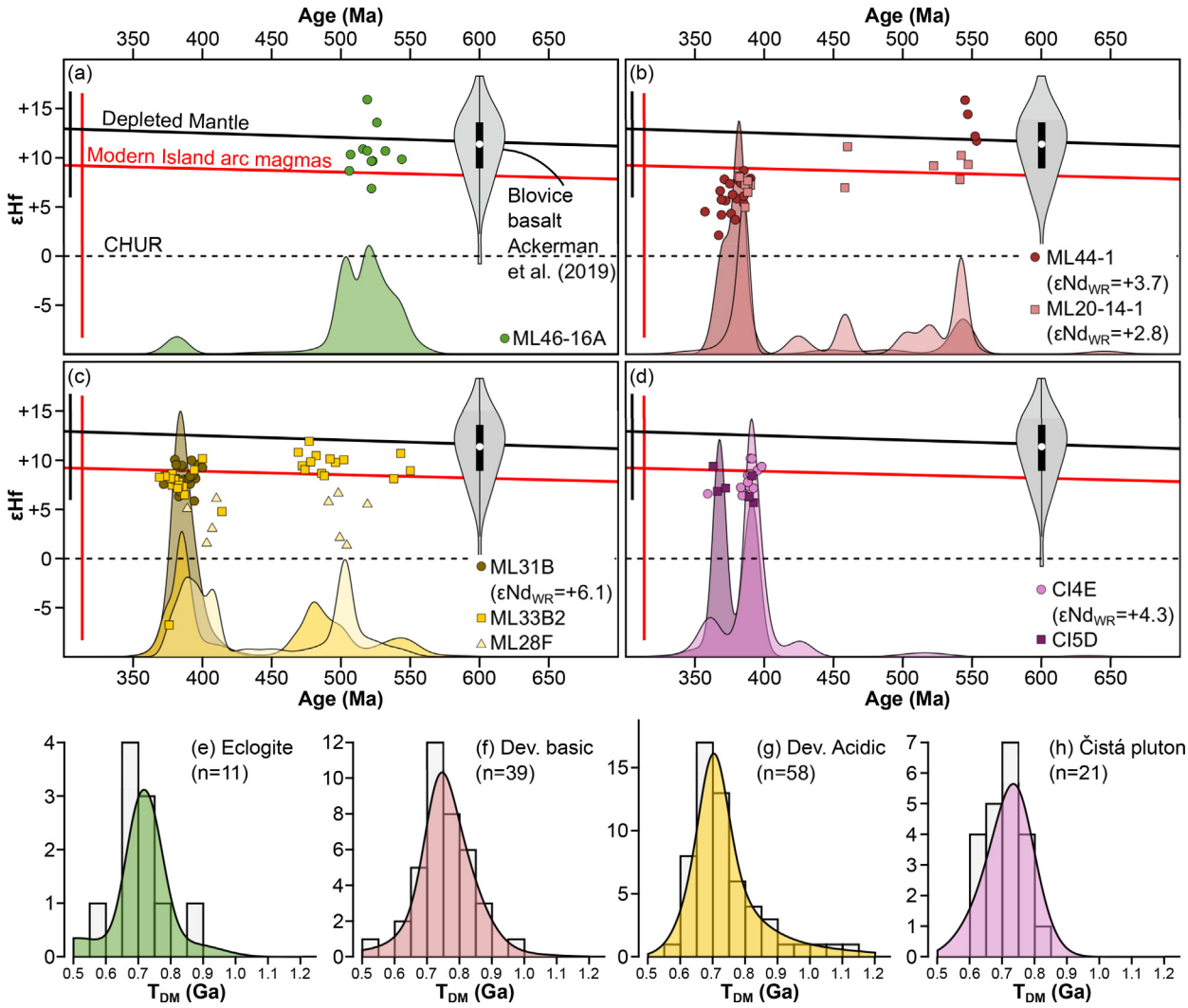

Fig. 7. Zircon Hf isotopic data from (a) eclogite, (b) basic Devonian magmatic rocks, (c) acidic Devonian magmatic rocks, and (d) upper plate Čista pluton. The Depleted Mantle line (thick black) is after Griffin et al. (2000) and Belousova et al. (2010), the composition of CHUR (dashed black) from Blichert-Toft and Albarède (1997). An evolution line for the average mantle source to modern island-arc magmas (thick red), as well as intervals $\varepsilon_{Hf}(t)$ of modern Mid-Ocean Ridge Basalt (MORB) and Island-Arc Basalts (corresponding vertical lines) are from Kemp and Hawkesworth (2014), a violin plot of whole Hf isotopic data from the basalt of the Blovice Accretionary Complex (Ackerman et al., 2019) is plotted for comparison. (e–h) Histograms and kernel density estimates for calculated two-stage time to depleted mantle (T_{DM}) model ages for different lithologies, details of calculations provided in the text.

late Devonian domains (n = 4) yield a weighted mean of +7.6 ± 0.3, indicating strong isotopic coherence regardless of U–Pb age (Fig. 7d). These data correspond to calculated T_{DM} crustal ages of 0.61 – 0.82 Ga with a weighted mean of 0.72 Ga (Fig. 7h).

5. Discussion

Based on the presented new zircon U–Pb and Hf isotopic data as well as the review of literature geochemical, isotopic and geochronological data published so far, it is evident that the Mariánské Lázně Complex (MLC) is composed of diverse protoliths exhibiting contrasting geochemical, chronological and metamorphic records. In spite of this the isotopic signatures observed in zircon Hf data and partially also in whole rock Nd isotopic data are remarkably homogeneous and additionally show strong coherence with magmatic rocks from the overlying Teplá-Barradian Zone (Fig. 8). This suggests that both the Cambrian and Devonian magmatic protoliths of the MLC were extracted from the same mantle source, which had already been modified during the Neoproterozoic. Moreover, this mantle source was additionally shared with the magmatic rocks of the Teplá-Barrandian Zone, which formed the upper plate with respect to the MLC during Devonian subduction/accretion. The implication of this finding is that the mantle lithosphere involved in this early stage of the Variscan Orogeny did not originate in the late Cambrian-Devonian age Rheic Ocean, but was instead captured from an older oceanic tract. In the following sections potential geodynamic settings for the protoliths of the MLC are discussed along with larger-scale paleogeographic considerations to present a generalised model for the reconstruction of the Mid-Devonian active margin of the European Variscan Belt.

5.1. From late Neoproterozoic (Cadomian) accretionary orogen to early Paleozoic Rheic Ocean opening

At least some parts of the MLC, principally those that bear no evidence for HP metamorphism, must have formed the lowermost part of Teplá-Barrandia prior to Devonian subduction/accretion (Peřestý et al., 2020). This is exemplified by the geochemical-petrological similarity of late Cambrian meta-gabbro in both the gabbro amphibolite zone of the MLC and in Teplá-Barrandia (e.g.,

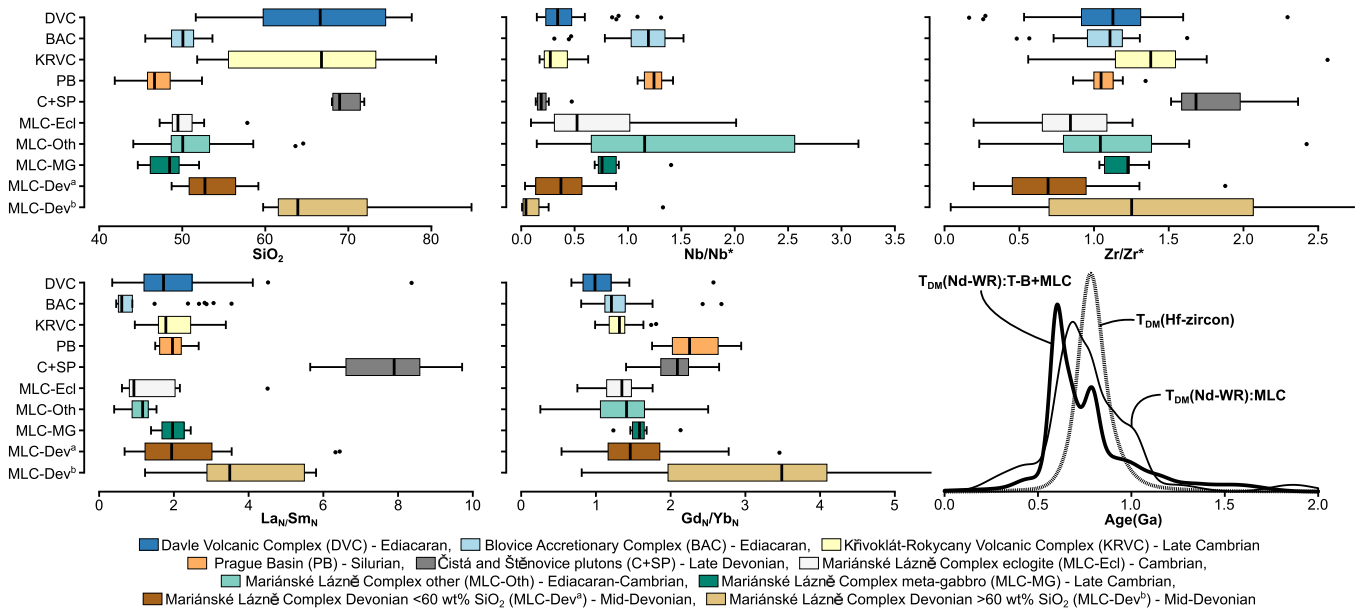

Fig. 8. Comparison of the chemical isotopic variation in magmatic rocks from the MLC and overlying Teplá-Barrandian zone. Definitions of chemical ratios are presented in caption to Fig. 3. Data compiled from: Ackerman et al. (2019); Beard et al. (1995); Crowley et al. (2002); Deiller et al. (2021); Drost et al. (2004); Jašarová et al. (2016); Pin et al. (2007); Santolík (2021); Tasáryová et al. (2018); Timmermann et al. (2004); Žák et al. (2011). Refer to Supplementary Data A for complete dataset.

Jašarová et al., 2016). The Neoproterozoic to Early Paleozoic reconstruction of Teplá-Barrandia has been widely discussed in recent years (e.g., Hajná et al., 2017, 2018; Ackerman et al., 2019; Žák et al., 2020). These works establish Teplá-Barrandia as a vast Ediacaran-Cambrian accretionary complex (the Blovice Accretionary Complex) associated with a *c.* 610 – 560 Ma volcanic arc (Davle Volcanic Complex). The termination of accretionary processes in the Blovice Accretionary Complex is associated with transition from a compressional to extensional tectonic setting and assumed to occur in the early to mid-Cambrian (*c.* 527 Ma – Hajná et al., 2017) following development of Cambrian wedge-top basins and granitic plutonism in the western part of the Blovice Accretionary Complex in the vicinity of the present day MLC (Dörr et al., 2002; Drost et al., 2011; Hajná et al., 2018).

The metabasite which forms the host rocks for the gabbro amphibolite zone were likely accreted to the base of the BAC during the latter stages of accretionary tectonics, being scraped off the subducting oceanic plate and therefore are directly comparable to similar basalts within the Blovice Accretionary Complex (Ackerman et al., 2019). This view is consistent with the overlap in geochemical and isotopic compositions of these basalts and amphibolites of the MLC (Fig. 8).

Gabbro intruded the amphibolite of the gabbro-amphibolite zone and the lowermost part of the Blovice Accretionary Complex during the late Cambrian. Ackerman et al. (2019) had suggested that they could have formed as a result of a fixed mantle plume, which also produced the more alkali basalts within the Blovice Accretionary Complex. However, the meta-gabbro, do not show the extreme within-plate enrichment associated with plume-derived rocks (Fig. 3), and are perhaps better explained by a model of ridge incision or thermal upwelling following collapse of the former subduction system (e.g., Collett et al., 2020).

The protoliths of the eclogite-amphibolite zone are more enigmatic. Both the eclogite and amphibolite were emplaced during the Cambrian (Timmermann et al., 2004; this work) and have been highly metamorphosed during the Devonian prior to and coevally with the emplacement of Mid-Devonian magmatic rocks (Collett et al., 2018; Deiller et al., 2021). Previous works (e.g., Beard et al., 1995; Crowley et al., 2002; Timmermann et al., 2004) have assumed that the protoliths of the eclogite amphibolite zone range from light REE-depleted N-MORB to light REE-enriched E-MORB associated with a single parental magma. This is inconsistent with the presented heterogeneity in the geochemical, isotopic, and geochronological data from which both supra-subduction and mid ocean ridge (MOR) settings can be inferred. A significant number of both eclogite and amphibolite exhibit Nb-depletion, which is often considered diagnostic of a supra-subduction zone setting (e.g., Kelemen et al., 1993). These samples also exhibit depletion in other HFSE (Ti, Zr, and Hf) which is linked to the retention of rutile and zircon during partial melting of the down-going slab. The strong coupling in Nb and Zr depletion (Fig. 3d) precludes significant involvement of a decoupled reservoir (e.g., Upper Continental Crust). A correlation between greater Nb-depletion and increased LREE fractionation (e.g. Fig. 3f) is also consistent with a supra-subduction setting for at least some of the protoliths of the MLC eclogite. This conclusion is also supported by enrichment in LILE (e.g. Fig. 3h,i). Nonetheless, given the mobility of these elements, and the fact that all of the rocks of the MLC have experienced at least amphibolite-facies metamorphism, any inference form these elements must be considered carefully. Notably, all of these trends are more developed in the eclogite samples (Deiller et al., 2021; this work) than in the metabasite samples studied by Crowley et al. (2002). It is difficult to make a categorical conclusion in the absence of petrological information on the samples studied by Crowley et al. (2002); however, it appears that a greater part of the eclogites were emplaced in a supra-subduction setting, while the amphibolites were derived from a more typical MOR source.

It should also be noted here that recently published data from eclogite of the Münchberg Massif (Pohlner et al., 2021), which is often correlated to the MLC (e.g., Franke et al., 2017), shows similar immobile trace element geochemical and isotopic variations as the eclogite and amphibolite of the MLC. However, Pohlner and co-workers explained this variation in terms of magmatic differentiation of a singular parental MORB-type magma in a continental setting. This conclusion is supported by strong positive Eu anomalies and depleted HREE contents in samples exhibiting volcanic arc geochemical signatures (Pohlner et al., 2021). In contrast, eclogite

from the MLC with a volcanic arc signature exhibit little to no Eu anomaly and a trend of increasing REE contents in comparison to the samples with a mid ocean ridge signature (Fig. 9). This suggests that while a single parental magma may be valid for the Münchberg Massif eclogite, the MLC eclogite is better explained by the aforementioned bimodal setting. In fact, an equivalent of the supra-subduction eclogite in the MLC may be present in the Münchberg Massif in the form of the more basic rocks of the Hangend Series at the top of the nappe pile (Koglin et al., 2018; Fig. 9). These rocks also exhibit supra-subduction geochemical signatures and U–Pb zircon geochronology yields similar Early Cambrian protolith ages. The reasons for this apparent contrast between the MLC and the Münchberg Massif are discussed in the section on Variscan evolution below.

The above indicates that the early Paleozoic architecture of the MLC-Teplá-Barrandian system must have been represented by a Cambrian volcanic arc (supra-subduction type eclogite/metabasite in MLC) separated from an Ediacaran arc and Ediacaran-Cambrian accretionary complex (Teplá-Barrandia) by a (sub-) oceanic basin (mid-ocean ridge type eclogite/metabasite in MLC). The chemistry of the sample dated in this study (ML46-16A) is ambiguous, but, depletion in HFSE (Nb_N/La_N ratios of 0.74 and Zr/Zr* ratio of 0.78) suggest some involvement of supra-subduction modified mantle. The spread in zircon U–Pb ages, including Ediacaran inheritance, and in the Lu-Hf isotopic signature ($\varepsilon_{Hf}(t)$ = +6.9 to +15.9) favours a back-arc or immature rift setting, established on juvenile Neoproterozoic crust. Additionally, the minimum emplacement age (*c.* 495 Ma) is similar to the assumed age of Münchberg Massif eclogite. The previous *c.* 540 Ma ages from Timmermann et al. (2004) date a slightly Nd depleted eclogite sample ($\varepsilon Nd_{(i)}$ = +6.8), a more enriched ($\varepsilon Nd_{(i)}$ = +2.5) amphibolite, and an intermediate granulite with adakitic-like chemistry, and can therefore be assumed to date the volcanic arc. An additional sample of eclogite, with more depleted ($\varepsilon Nd_{(i)}$ = +7.7) composition had only a single *c.* 500 Ma zircon (Timmermann et al., 2004), and may therefore be equivalent to the sample studied in this work.

Nonetheless, this indicates chronological overlap between termination of accretionary tectonics in Teplá-Barrandia and the establishment of the MLC volcanic arc necessitating two discrete subduction zones established on isotopically similar Neoproterozoic sub-oceanic lithospheric mantle (SOLM). Ackerman et al. (2019) already proposed a similar scenario in order to explain supra-subduction zone signatures in the basalt of the Blovice Accretionary Complex. The model of Ackerman et al. (2019) assumes a Western Pacific type scenario with steep subduction of a Mid-Proterozoic (Mirovoi?) oceanic crust forming a hypothetical arc and back arc basin, with shallow subduction of the back-arc forming the juvenile Neoproterozoic volcanic arc and Ediacaran-Cambrian accretionary complex of Teplá-Barrandia (Fig. 10). In this view, the hypothetical arc would be an embryonic stage of the future MLC volcanic arc. However, many models for the wider Avalonian-Cadomian orogeny prefer an Eastern Pacific style system (e.g., Nance et al., 2002), where young oceanic crust of an old (Mirovoi?) spreading centre is subducted to form the Ediacaran volcanic arc (Fig. 10). In this scenario the second subduction zone must develop behind the original spreading centre to form the Cambrian MLC volcanic arc. In both scenarios, the basin separating the two arc systems would be originally late Neoproterozoic to early Cambrian in age and may involve Cambrian back-arc intrusions, which are an additional potential source of the mid-ocean ridge type eclogite/metabasite in MLC.

5.1.1. Paleogeographic considerations

Teplá-Barrandia and the MLC form part of the wider Avalonian-Cadomian belt, which developed on the margin of the East European, Amazonian, and West African cratons in the Neoproterozoic (e.g., Nance and Murphy, 1994). Most paleogeographic models do not account for the presence of a Cambrian age volcanic arc within the Cadomian segment. However, the presence of a Cambrian age volcanic arc is not restricted to this work; it is a well-documented feature of the uppermost allochthonous complexes in NW Iberia (Andonaegui et al., 2016), which are correlated through the allochthonous complexes of Armorica (e.g., Ballèvre et al., 2014) and possibly also in the French Massif Central (e.g., Berger et al., 2010; Lardeaux et al., 2014) or the External Crystalline Massifs of the Western Alps (e.g., Guillot and Ménot, 2009). Correlation between the Variscan metamorphic evolution of these allochthonous complexes with the MLC and other Mid-Devonian metamorphic complexes of the Bohemian Massif is firmly established (e.g., Martínez Catalán et al., 2020, 2021). Within the Bohemian complexes, both Koglin et al. (2018) and Tabaud et al. (2021) present evidence for active margin sedimentation until the late Cambrian.

Recently, Merdith et al. (2021) presented a full plate paleogeographic model for the past 1000 Myr. In their model, they suggest a subduction zone outboard of the Cadomian terranes in the Cambrian in order to accommodate the late Ediacaran to Cambrian movement of the East European Craton (Baltica). Baltica occupied southerly latitudes proximal to the West African Craton, and by extension the Avalonian-Cadomian Belt until *c.* 580 Ma (Fig. 11a). Rifting, associated with the opening of the Iapetus Ocean, transported Baltica to equatorial latitudes (Fig. 11b). However, during

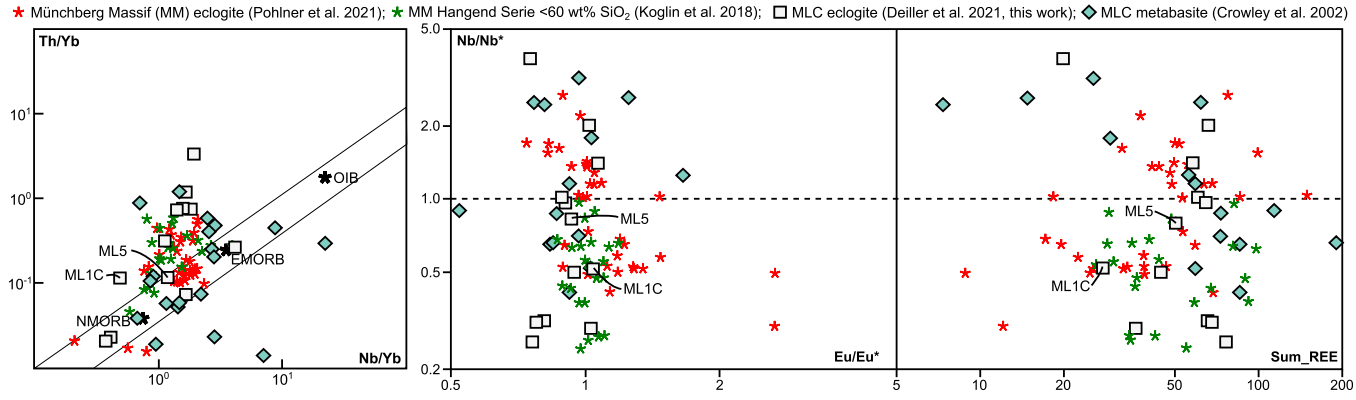

Fig. 9. Comparison of geochemical data from MLC and Münchberg Massif (Koglin et al., 2018; Pohlner et al., 2021). While eclogite from both complexes appear to have both mantle-derived and supra-subduction members in the Nb/Yb vs Th/Yb classification diagram (Pearce, 2008); the supra-subduction-type (Nb/Nb* <1) from the Münchberg Massif are characterised by increasing Eu anomaly (Eu/Eu*) and decreasing total REE contents. Pohlner et al. (2021) link this to their cumulate origin, while no such correlation exists for the MLC rocks. A better correlation therefore may be the Early Cambrian supra-subduction rocks in the Hangend Serie of the Münchberg Massif.

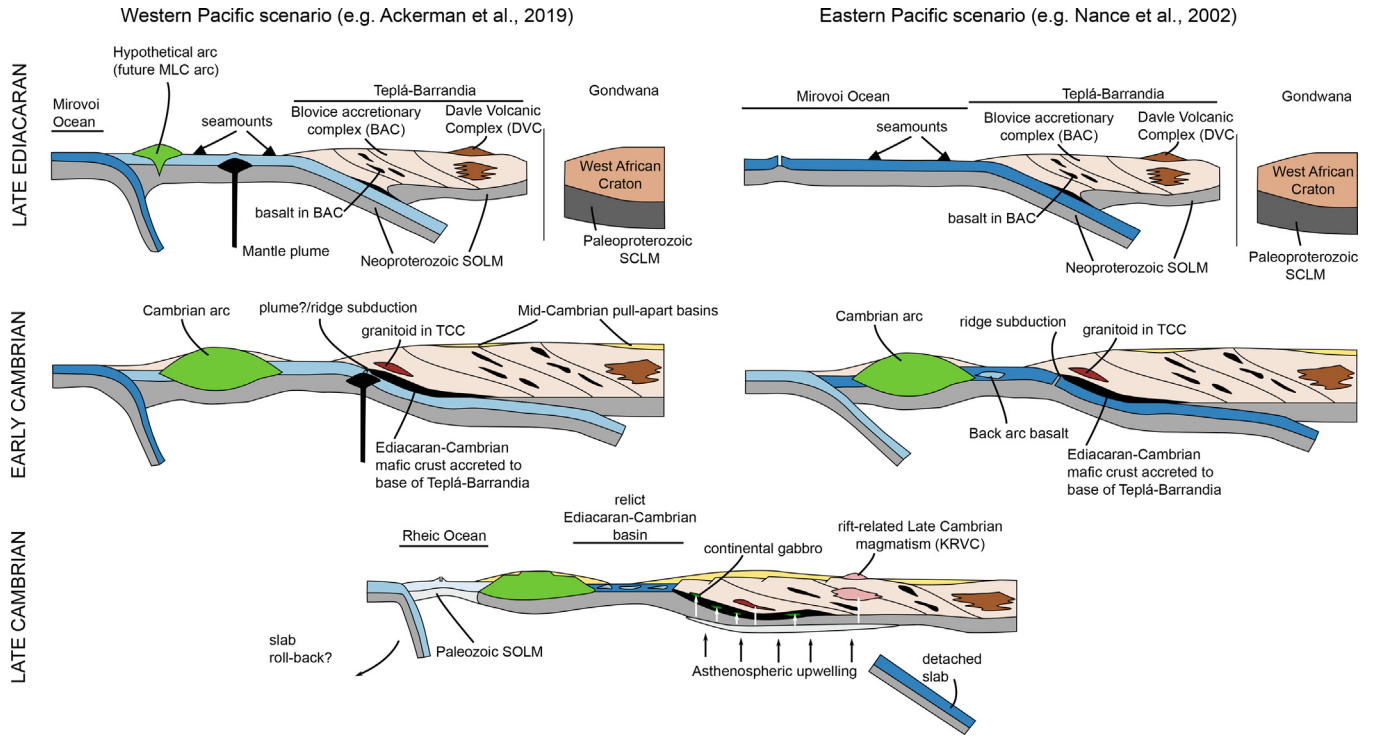

Fig. 10. Geodynamic evolution of the MLC-Teplá-Barrandia system during the Late Ediacaran to Late Cambrian, two end-member possibilities are presented either as a Western Pacific scenario (after Ackerman et al., 2019) or in an Eastern Pacific scenario (after Nance et al., 2002). Both models end up with a similar situation in the Late Cambrian with the main difference being whether the relict Ediacaran-Cambrian basin captured between the MLC arc and Teplá-Barrandia originally belonged to a back-arc basin or from MORB-type crust of the Mirovoi Ocean spreading centre.

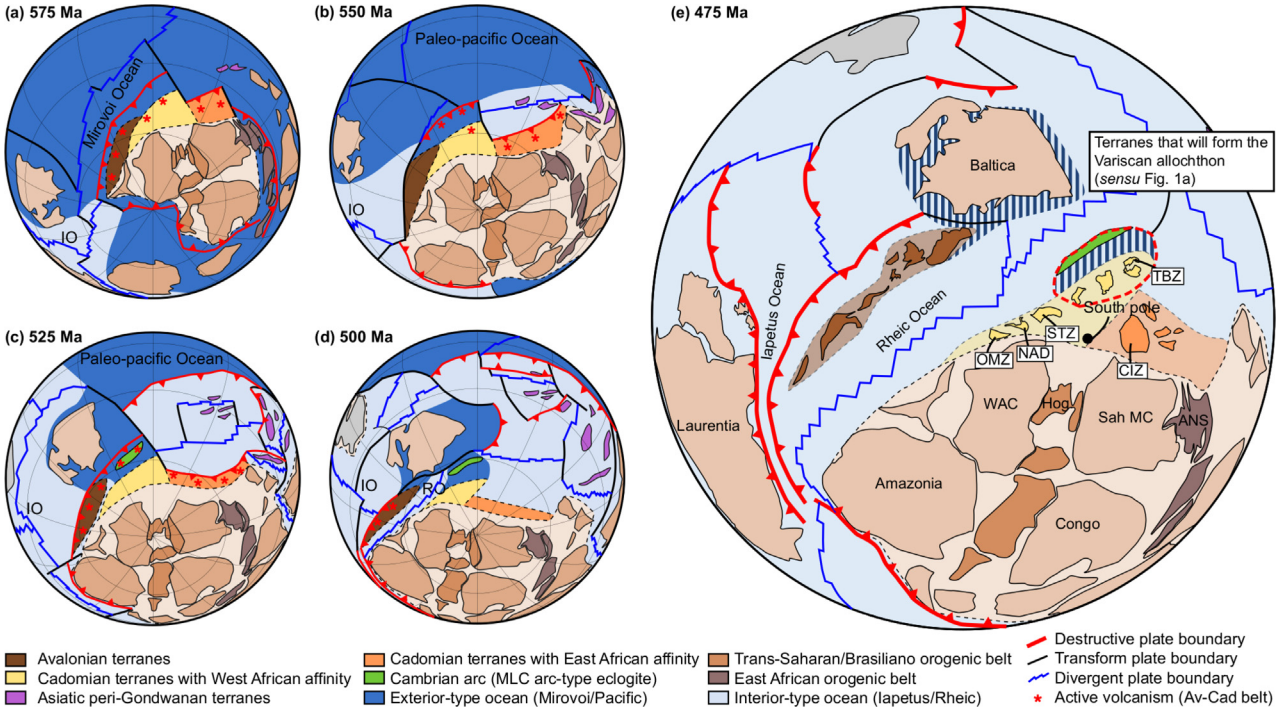

Fig. 11. Paleogeographic reconstructions after Merdith et al. (2021) for the Late Ediacaran to Early Ordovician. The hatched segments in (e) represent relics of Mirovoi-type oceanic lithosphere captured during opening of the Iapetus (IO) and Rheic (RO) Oceans.

the Cambrian, Baltica drifted back towards the now amalgamated Gondwana landmass necessitating the aforementioned subduction zone outboard of the Avalonian-Cadomian Belt (Fig. 11c), which consumes much of the relic oceanic basin north of these terranes (see fig. 18 in Merdith et al., 2021). In drawing this subduction zone, Merdith et al. (2021) noted that while the Ganderian arc in the Avalonian segment accounted for this, they were unaware of an equivalent in the Cadomian sector. However, from the existence

of a Cambrian arc, which is today preserved in high-grade metamorphic complexes spanning Iberia to Bohemia is a first order evidence in support of such a model.

Intriguingly, the input of Baltica-derived material into the Cambrian arc was already proposed for the NW Iberian segment by Henderson et al. (2016) on the basis of overlapping linear εHf-time arrays in late Archean and early Paleoproterozoic zircon. Additionally, the present-day southern margin of Baltica, which according to the model of Merdith et al. (2021) was facing this Cambrian arc, contains sedimentary input from an as yet unidentified Cambrian age volcanic arc (e.g., Paszkowski et al., 2021).

5.1.2. Opening of the Rheic Ocean

The next phase of the model relates to the opening of the Rheic Ocean in the Late Cambrian through Early Ordovician (e.g., Nance et al., 2010, 2012). The opening of the Rheic Ocean separated the Avalonian and Cadomian segments of the Avalonian-Cadomian Belt (Fig. 11d, e) and has been interpreted to have developed from pull-apart basins following the aforementioned ridge incision (e.g., Linnemann et al., 2004) or alternatively as an evolved back-arc in a slab-rollback setting (e.g., Martínez Catalán et al., 2007). Although some earlier works in NW Iberia had located the Rheic Suture between the Cambrian arc defined above and the peri-Gondwanan terranes (e.g., Martínez Catalán et al., 2007); it is now generally accepted (e.g., Arenas et al., 2014; Díez Fernández et al., 2020) that the Rheic Ocean opened in front of the Cambrian arc. A slab-rollback setting is compatible with the presented model, whereby progressively older and denser oceanic crust of the Baltica passive margin is introduced into the subduction zone and this rollback may have contributed to extension and Ordovician high temperature – low pressure (HT-LP) metamorphism observed in the peri-Gondwanan terranes (e.g., Peřestý et al., 2017); although, it could also be partially explained by the collapse of the former Mirovoi Ocean subduction system (e.g., Fig. 10; Collett et al., 2020). Ordovician generation of new gabbroic/basaltic crust within the proposed relic oceanic basin has been identified in other segments of the European Variscan Belt (e.g., Paquette et al., 2017; Sánchez Martínez et al., 2021). While the Mid-Devonian magmatic rocks of the MLC contain inherited zircon of this age, no new Ordovician crust has thus far been recognised in the MLC. Intriguingly, in both the Iberian (Sánchez Martínez et al., 2021) and Armorican (Paquette et al., 2017) examples, this Ordovician crust is associated with re-working of Stenian age crust, comparable to the oldest T_{DM} model ages presented here (Fig. 6) and perhaps further supporting the notion that this basin was inherited from the Mirovoi Ocean.

Within the MLC-Teplá Barrandian system, Peřestý et al. (2017) identified the Ordovician HT-LP event in the Teplá Crystalline Complex by U–Pb monazite dating from low-Ca garnet cores, overprinted by Variscan Barrovian metamorphism. In the MLC, Faryad (2012) also identified relic cores in eclogitic garnet with unusual low Ca compositions. Although Faryad (2012) interpreted these as evidence for two high-pressure events, the P–T conditions are imprecisely constrained and the composition of the garnet is more consistent with a HT-LP metamorphism. Likewise, a similar evolution of firstly HT-LP and later HP metamorphism is documented in eclogite from the Southern Armorican Massif (e.g., Godard, 2010), which also forms part of the Variscan allochthon (Fig. 1a) of Martínez Catalán et al. (2021). It is not clear what was the whole rock composition of the samples studied by Faryad (2012); however, samples in this study from the same locality have depleted N-MORB type compositions, suggesting they may have belonged to the relic oceanic basin rather than the Cambrian arc. Nonetheless, it appears that this extensional event did not significantly modify the lithospheric mantle beneath the MLC-Teplá-Barrandia system, as evidenced by the paucity of post-Cambrian juvenile zircon, and can therefore be assumed to be distal from the opening of the Rheic Ocean (Fig. 10).

5.2. Variscan evolution of the MLC-Teplá-Barrandia system

The earliest record of convergence related to the Variscan Orogeny is the Mid-Devonian high-pressure metamorphism that can be traced from the allochthonous complexes in NW Iberia, through the Southern Armorican Massif, and the French Massif Central to the MLC and similarly aged high-pressure complexes in the Bohemian Massif (e.g., Martínez Catalán et al., 2020, 2021). Assuming normal rates of subduction, in order to accommodate eclogite-facies metamorphism by *c.* 400 Ma, then subduction must have already initiated in the late Silurian. In Teplá-Barrandia, the Silurian is characterised by an important phase of rift related (ultra-) mafic magmatism (Tasáryová et al., 2018). Tasaryová and co-workers linked this magmatism to far field forces associated with final closure of the Iapetus Ocean and the Caledonian Orogeny. This time period is also associated with development of arc magmatism on the southern margin of the now amalgamated Laurussian landmass (e.g., Franke, 2000; Zeh and Will, 2010). These far-field events likely acted as push/pull forces initiating subduction in and around the peri-Gondwanan terranes. As the site of the oldest (densest) oceanic crust the proposed relict Ediacaran-Cambrian basin represents the most likely site for this subduction initiation (Fig. 12).

For the allochthonous complexes in NW Iberia and Armorican Massif, subduction is typically assumed (e.g., Arenas et al., 2014; Ballèvre et al., 2014; Díez Fernández et al., 2020) to have been directed beneath the Cambrian arc from the south (i.e., peri-Gondwana is subducted beneath the Cambrian arc) and continuous into the Early Carboniferous. However, within the study area, rocks of the Cambrian arc crop-out beneath peri-Gondwana (Teplá-Barrandia), necessitating opposing subduction polarity. The models of Martínez Catalán et al. (2020, 2021) circumvent this problem by assuming that all of the terranes that form the Variscan allochthon (Fig. 1a) belonged to a single coherent terrane prior to the Variscan Orogeny (i.e., that Teplá-Barrandia can be directly correlated with the Cambrian arc in Iberia). However, early Cambrian termination of accretionary tectonics in Teplá-Barrandia and late Cambrian rift-related volcanics (Křivoklát-Rokycany volcanic complex (KRVC) – Fig. 9) appears incompatible with an active volcanic arc in the late Cambrian in NW Iberia (Andonaegui et al., 2016). Additionally, to accommodate the opposing subduction polarity in present-day co-ordinates, Martínez Catalán et al. (2021) require Carboniferous orocline-like bending of the Variscan allochthon.

Alternatively, if we assume that Teplá-Barrandia belongs to the peri-Gondwanan shelf (Fig. 11e), then opposing subduction polarity must already have been established in the Devonian. This can be accommodated through oblique convergence and transform faults as envisaged in Fig. 12. Oblique convergence and transform faulting additionally allows for the opening of Devonian pull-apart basins within the relict Ediacaran-Cambrian basin, from which would form Devonian age ophiolites (e.g., Kryza and Pin, 2010; Arenas et al., 2014). Many of these Devonian ophiolites have anomalously enriched or depleted Nd isotopic compositions, which may further support their formation on a relict Proterozoic basin (e.g., Murphy et al., 2011).

Subduction is initially oceanic and consists of the remnant oceanic crust of the Ediacaran-Cambrian basin. For the MLC, this subduction could be represented by the sample ML5 with MORB-type chemistry, (Nb/Nb^* = 0.83, Z/Zr^* = 1.08, εNd = +7.4), and a Lu–Hf garnet age of *c.* 390 Ma. However, for MORB-type eclogite in the correlated Münchberg Massif (Pohlner et al., 2021), HP conditions were potentially reached earlier (*c.* 400 Ma – Koglin et al., 2018 and references therein). The exhumation of these eclogites

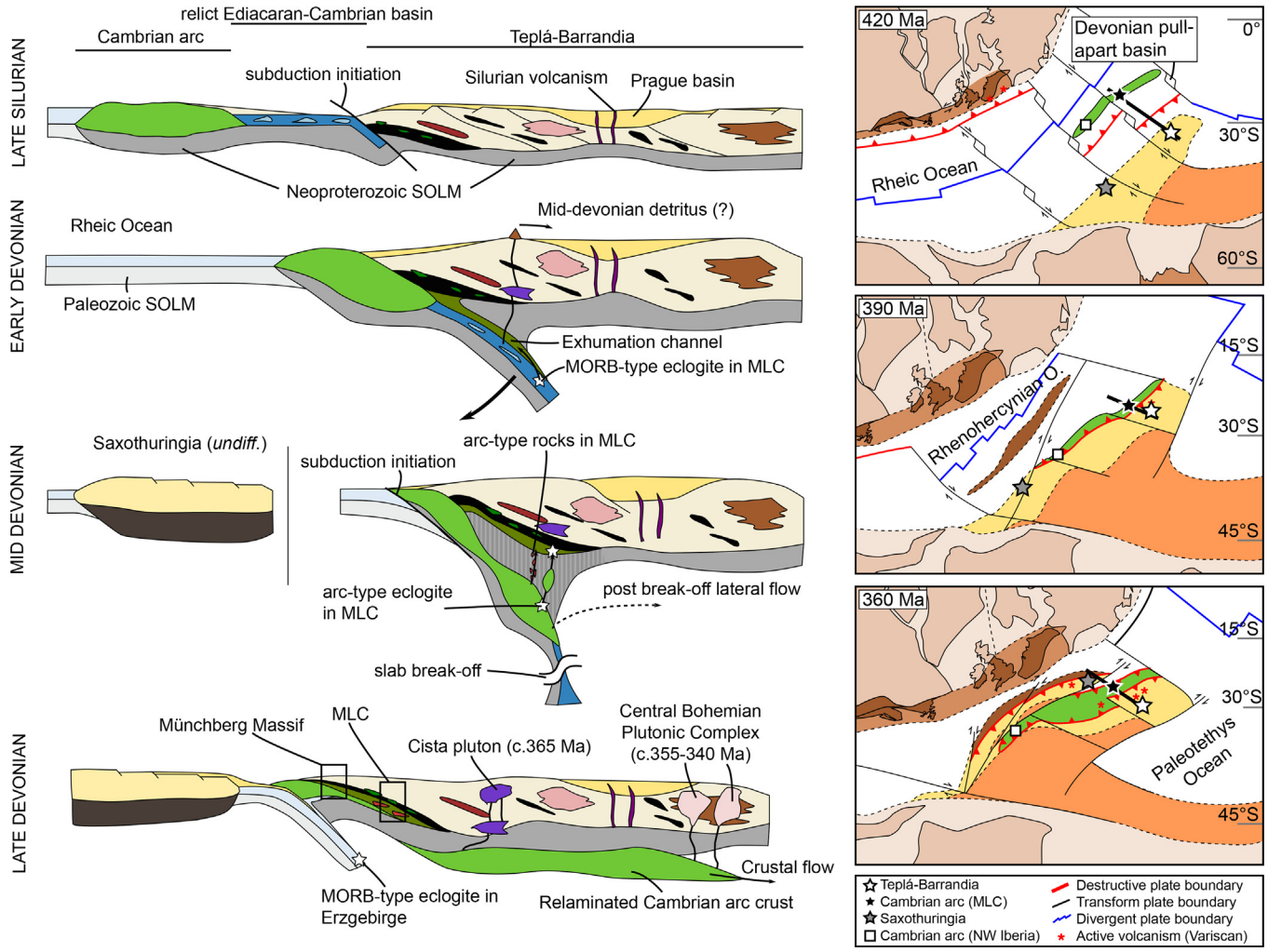

Fig. 12. Late Silurian to Late Devonian geodynamic evolution of the MLC-Teplá-Barrandia system. Main stages are represented by plate-scale cross-sections (left) and map view reconstructions (right). Original architecture in the plate-scale cross-sections follows that of Fig. 10. The map view snapshots are adapted from reconstructions in Merdith et al. (2021), the original position of terranes and oceanic basins follows logic in Fig. 11e, white star represents Teplá-Barrandia, black star – volcanic arc elements in MLC, grey star – Saxothuringia, and white square the allochthonous complexes in NW Iberia.

likely occurred within a relatively simple channel flow setting and may have partially under-plated the upper plate (e.g., Gerya et al., 2002; Warren et al., 2008; Fig. 12-Early Devonian). This subduction may also be responsible for deep crustal magmatism from which the large population of inherited Early to Mid-Devonian zircon was observed in the Čistá Pluton (Deiller et al., 2021).

The second phase of the model requires deep subduction of the Cambrian arc. The question of whether buoyant arc-crust can be subducted has previously been hotly debated (e.g., Cloos, 1993). Three features of the Cambrian arc are likely to aid its subduction, firstly its age (*c.* 80 – 120 Myr older than subduction) allows for significant cooling and densification to have taken place, secondly relics of dense Ediacaran-Cambrian oceanic lithosphere likely acted as an anchor pulling the arc-crust down, and finally Early Ordovician extension may have significantly thinned the arc crust, all of which enables arc subduction, as shown in experiments of Boutelier et al. (2003). Additionally, these experiments indicate that any weakness within the arc may be exploited, favouring subduction of more mafic material over more felsic, explaining the limited extent of felsic crust belonging to the Cambrian arc present in the MLC.

The type sample for arc-type crust in the MLC is the ML1C sample (Nb/Nb* = 0.52, Zr/Zr* = 0.92, εNd = +5.0); this sample yielded a Lu–Hf garnet age of *c.* 382 Ma (Collett et al., 2018). Although the Lu–Hf dates may represent minimum age for the eclogite-facies event (as discussed in Collett et al., 2018), this would suggest exhumation must have been rapid in order to allow for granulite-facies overprint by *c.* 380 Ma (Timmermann et al., 2004; U–Pb data presented in this article). One way such a rapid exhumation could be achieved is by diapiric ascent (e.g., Hall and Kincaid, 2001; Yin et al., 2007; Fig. 12-Mid Devonian), which is compatible with the introduction of more buoyant volcanic arc material into the subduction zone. Ascent of initially cold diapirs through a hot mantle wedge also allow for the granulite-facies overprint documented in eclogite (e.g., Collett et al., 2018), which is notably not observed in the Münchberg Massif eclogite (e.g., O'Brien, 1997).

Subduction of the Cambrian volcanic arc and a diapiric model of exhumation may also explain the occurrence of contemporaneous magmatic rocks in the MLC (Deiller et al., 2021). These rocks have strong Nb depletion (Fig. 3), compatible with a supra-subduction setting, but variable Zr depletion/enrichment indicates decoupling of the HFSE. While this may indicate assimilation of a HFSE decoupled reservoir (e.g., Upper Continental Crust), it more likely reflects the presence of amphibole in the source capable for HFSE fractionation (e.g., Tiepolo et al., 2001). While the observed strong REE

fractionation may also be controlled by presence of amphibole and/or garnet (e.g., Alonso-Perez et al., 2009). The relative involvement of either amphibole or garnet can be tested using Dy/Dy* parameter defined by Davidson et al. (2013). Theoretically amphibole (and clinopyroxene) fractionation should be correlated with decreasing Dy/Dy*. In the case of amphibole decreasing Dy_N/Yb_N ratios; the presence of garnet may either increase or decrease Dy/Dy*, but will lead to significant increase of Dy_N/Yb_N ratios. In Fig. 13a it can be recognised that the presence of amphibole likely influences some of the more basic samples; however, the presence of garnet becomes more significant for the more acidic samples. Nonetheless, some amphibole (±magnetite) control for all samples can be assumed on the basis of progressively developing negative Ti anomalies (Fig. 13b). Considering the lack of juvenile Devonian age zircon presented here and overlap in isotopic composition with the retrogressed eclogite (Fig. 7) the data are compatible with a model of melting of portions of the subducted Cambrian volcanic arc and limited involvement of a juvenile depleted mantle. Deiller et al. (2021) had already inferred melting of an older volcanic arc source for the felsic magmatic rocks on the basis of geochemical modelling; however, the results here extend that conclusion also to the more mafic magmatic rocks. Thermomechanical modelling of diapiric exhumation indicates that larger and faster moving diapirs will preserve metamorphic assemblages while smaller and slower diapirs will become molten contributing to arc volcanism (Yin et al., 2007). Therefore, the Devonian magmatic rocks may represent partially molten parts of eclogitic diapirs derived from the Cambrian volcanic arc.

Further perspective on such a model can be gained from considering the Góry Sowie Massif; another Mid-Devonian HP complex of the Bohemian Massif. Unlike the MLC (or the Münchberg Massif), HP rocks are predominantly intermediate-felsic composition with only few mafic eclogite of apparent volcanic arc affinity (Kryza and Fanning, 2007; Tabaud et al., 2021). The Góry Sowie Massif is also characterised by a high temperature granulite-facies metamorphism and therefore, following the proposal given above, it would represent a portion of the Cambrian arc that exhumed diapirically. This is consistent with the rim of unmetamorphosed and weakly deformed Sudetic Devonian ophiolites (e.g Kryza and Pin, 2010). For the presented model to work, the Góry Sowie Massif must have originally formed as a dome intruding Teplá-Barrandia, which is locally represented only by the Kłodzko Unit, which overlies the Devonian ophiolites (e.g., Aleksandrowski and Mazur, 2002; Mazur et al., 2004). Although equivalents of the Devonian ophiolites are not defined in the MLC section, one possibility is that the serpentinite body, rather than being an integral part of the MLC as described in Kastl and Tonika (1984) and Jelínek et al. (1997), is instead part of the Kladská unit (Kachlík, 1993). This view is consistent with field relations where serpentinite additionally crops out in small bodies within the Kladská unit metabasites (Fig. 1c). The geochemical signature of the serpentinite is best comparable to that of subducted serpentinites with relatively high Ti (>0.02 wt. % TiO_2) and Yb (0.05 to 0.28 ppm) content, flat REE patterns and lack of Eu anomaly (Deschamps et al., 2013). Nonetheless, there is only evidence for a medium-temperature metamorphism (replacement of spinel by chlorite and diopside by tremolite – Medaris et al., 2011) comparable to the metamorphism recorded in the Kladská unit. The age of the Kladská metabasites is not constrained, but the Kladská unit occupies a similar position to the Devonian ophiolites in the Sudetes and thus a similar tectonic setup may be expected.

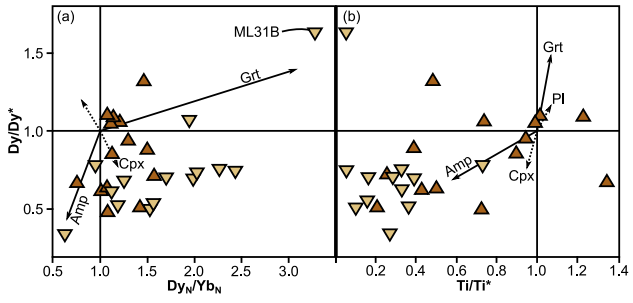

Fig. 13. Binary plots underlining the important petrogenetic role played by amphibole and garnet in Devonian magmatic rocks (symbols as in Fig. 3). Dy/Dy* and Ti/Ti* after Davidson et al. (2013) and Janoušek et al. (2018), normalisation to CI chondrite (Boynton, 1984). Mineral vectors represent fractional crystallisation trends for single minerals from primitive mantle following Janoušek et al. (2018).

Nonetheless, if the presented model is valid, then the early Variscan HP complexes of the Bohemian Massif each preferentially sample different segments of the subduction-exhumation system. The Münchberg Massif is the oldest and samples predominantly mid-ocean ridge-type basaltic rocks and less subducted parts of the Cambrian arc (i.e., Hangend Serie – Koglin et al., 2018) exhumed within a channel flow system; the MLC samples both MOR-type basalts exhumed within the channel and more mafic parts of the Cambrian arc exhumed diapirically; while the Góry Sowie Massif dominantly samples more felsic parts of the Cambrian arc exhumed diapirically as a dome beneath the upper plate Teplá-Barrandian Zone and Sudetic ophiolites.

Renewed oceanic subduction behind the Cambrian arc is necessary to explain Late Devonian to Early Carboniferous oceanic blueschist and eclogite in the southern margin of Saxothuringia (Schmädicke et al., 1995; Konopásek et al., 2019; Fig. 12: Mid Devonian and Late Devonian). Moreover, the present configuration of the Variscan belt requires that peri-Gondwanan crust (i.e., Saxothuringia within the Bohemian Massif) is translated into this zone behind the Mid-Devonian subduction/accretion system. To fit the presented model, this must be achieved through NE-SW (present co-ordinates) dextral shearing along the peri-Gondwanan margin. NE-SW shearing is well documented in the Carboniferous of the Variscan Belt and is integral to the model presented in Martínez Catalán et al. (2021). However, in order to fit the geological record in the Bohemian Massif, then shearing must be earlier, as the continental margin of Saxothuringia is subducted to UHP depths already at *c.* 350 Ma (e.g., Závada et al., 2021). This scenario is already envisaged in models of Franke and Żelaźniewicz (2002), who identify NE-SW dextral shearing between the Bohemian terranes already at 380 Ma. The origin of this shearing fits within the model of oblique subduction beneath the peri-Gondwanan margin, creating transpressional forces which decouple a piece of peri-Gondwana moving it dextrally along the margin. If true, then these movements would appear to parallel the Silurian-Devonian dominantly sinistral movements that occur within the Laurussian terranes (e.g., Hutton, 1987; Dewey and Strachan, 2003; Fig. 12). Thus, representing a form of strike-slip duplication similar to that documented in other large-scale Phanerozoic accretionary systems (e.g., Lachlan Orogen – Glen et al., 1992; Central Asian Orogenic Belt – Şengör et al., 1993).

A corollary of this presented model is that the relaminant, which models of Schulmann et al. (2009, 2014), Maierová et al. (2021) and others propose will go on to form HP granulite domes within the Moldanubian Zone of the Bohemian Massif was likely composed of the Cambrian arc crust; potentially also partially molten during the Mid-Devonian. This inference is consistent with late Cambrian inheritance in zircon from HP granulite as well as presence of cryptic 400–360 Ma dates (e.g., Janoušek et al., 2006b; Nahodilová et al., 2014; Kusbach et al., 2015; Štípská et al., 2016); although late Cambrian inheritance is not diagnostic of this model since such ages are widespread in the Variscan Belt (e.g. Pin

et al., 2007). Nonetheless, Lu–Hf garnet geochronology of mantle-derived rocks associated with the HP granulite domes indicates that they were subducted already in the Devonian (e.g., Ackerman et al., 2020). And the data presented by Ackerman et al. (2020) also provides the final piece of evidence suggesting that the early Variscan subduction was associated with an old Neoproterozoic basin, as Re–Os isotopic data suggest that this mantle had experienced a Neoproterozoic partial melting event.

6. Conclusions

The European Variscan belt is characterised by distinct phases of HP metamorphism from the mid Devonian through to the Carboniferous. The mid-Devonian phase is characterised by HP-HT conditions that are not necessarily compatible with oceanic subduction of a vast Rheic Ocean domain. The Mariánské Lázně Complex in the Bohemian Massif is a valuable object in reconstructing the mid-Devonian phase of the Variscan Orogeny as it maintains structural continuum with its original upper plate (the Teplá Barrandian Zone). Review of whole rock geochemical and isotopic data reveals that Cambrian protoliths of the MLC were likely emplaced in a transitional volcanic arc-back arc setting. Combined with new zircon Hf isotopic data, it is proposed that they were established above a mantle source that had been enriched during the Neoproterozoic. Data from Devonian magmatic rocks, which intrude the MLC and Teplá Barrandian Zone, indicate that this mantle source was unaffected by Paleozoic opening of the Rheic Ocean. These data also indicate that the earliest phase of the Variscan Orogeny was associated with the closure of a relict Ediacaran-Cambrian basin, which had been captured from the Mirovoi Ocean and has important implications for the reconstruction of the whole European Variscan Belt.

Declaration of Competing Interest

The authors declare that they have no known competing financial interests or personal relationships that could have appeared to influence the work reported in this paper.

Acknowledgements

This study was funded by the Grant Agency of the Czech Republic (GAČR) project 19-25035S to P. Štípská and the International Partnership Program of CAS 773 (132744KYSB20190039) to Y. Jiang. Institutional supports of the Research Project no. 310760 (Strategic Research Plan of the Czech Geological Survey-DKRVO/ČGS 2018–2022) and Centre for Geosphere Dynamics (UNCE/SCI/006) of Faculty of Sciences, Charles University are gratefully acknowledged. The manuscript benefited from constructive reviews by S. Mazur (Polish Academy of Sciences) and an anonymous reviewer and R. Palin is thanked for editorial handling.

Appendix A. Supplementary data

Supplementary data to this article can be found online at https://doi.org/10.1016/j.gsf.2022.101374.

References

Ackerman, L., Bizimis, M., Haluzová, E., Sláma, J., Svojtka, M., Hirajima, T., Erban, V., 2016. Re–Os and Lu–Hf isotopic constraints on the formation and age of mantle pyroxenites from the Bohemian Massif. Lithos 256, 197–210. https://doi.org/10.1016/j.lithos.2016.03.023.

Ackerman, L., Hajná, J., Žák, J., Erban, V., Sláma, J., Polák, L., Kachlík, V., Strnad, L., Trubač, J., 2019. Architecture and composition of ocean floor subducted beneath northern Gondwana during Neoproterozoic to Cambrian: a palinspastic reconstruction based on Ocean Plate Stratigraphy (OPS). Gondwana Res. 76, 77–97. https://doi.org/10.1016/j.gr.2019.07.001.

Ackerman, L., Kotková, J., Čopjaková, R., Sláma, J., Trubač, J., Dillingerová, V., 2020. Petrogenesis and Lu–Hf dating of (ultra) mafic rocks from the Kutná Hora Crystalline Complex: implications for the Devonian evolution of the Bohemian Massif. J. Petrol. 61, egaa075. https://doi.org/10.1093/petrology/egaa075.

Agard, P., Yamato, P., Jolivet, L., Burov, E., 2009. Exhumation of oceanic blueschists and eclogites in subduction zones: timing and mechanisms. Earth-Sci. Rev. 92 (1-2), 53–79. https://doi.org/10.1016/j.earscirev.2008.11.002.

Aleksandrowski, P., Mazur, S., 2002. Collage tectonics in the northeasternmost part of the Variscan Belt: the Sudetes. In: Winchester, J.A., Pharaoh, T.C., Verniers, J. (Eds.), Palaeozoic Amalgamation of Central Europe. Geol. Soc. SP 201, 237–277. doi: 10.1144/GSL.SP.2002.201.01.12.

Alonso-Perez, R., Müntener, O., Ulmer, P., 2009. Igneous garnet and amphibole fractionation in the roots of island arcs: experimental constraints on andesitic liquids. Contrib. Mineral. Petr. 157 (4), 541–558. https://doi.org/10.1007/s00410-008-0351-8.

Andonaegui, P., Arenas, R., Albert, R., Martínez, S.S., Fernández, R.D., Gerdes, A., 2016. The last stages of the Avalonian-Cadomian arc in NW Iberian Massif: isotopic and igneous record for a long-lived peri-Gondwanan magmatic arc. Tectonophysics 681, 6–14. https://doi.org/10.1016/j.tecto.2016.02.032.

Arenas, R., Sánchez Martínez, S., Gerdes, A., Albert, R., Díez Fernández, R., Andonaegui, P., 2014. Re-interpreting the Devonian ophiolites involved in the Variscan suture: U-Pb and Lu–Hf zircon data of the Moeche Ophiolite (Cabo Ortegal Complex, NW Iberia). Int. J. Earth Sci. 103 (5), 1385–1402. https://doi.org/10.1007/s00531-013-0880-x.

Ballèvre, M., Martínez Catalán, J.R., López-Carmona, A., Pitra, P., Abati, J., Fernández, R.D., Ducassou, C., Arenas, R., Bosse, V., Castiñeiras, P., Fernández-Suárez, J., Gómez Barreiro, J., Paquette, J.-L., Peucat, J.-J., Poujol, M., Ruffet, G., Sánchez Martínez, S., 2014. Correlation of the nappe stack in the Ibero-Armorican arc across the Bay of Biscay: a joint French–Spanish project. Geological Society, London, Special Publications 405 (1), 77–113.

Beard, B.L., Medaris, L.G., Johnson, C.M., Jelínek, E., Tonika, J., Riciputi, L.R., 1995. Geochronology and geochemistry of eclogites from the Mariánské Lázně Complex, Czech Republic: implications for Variscan orogenesis. Geol. Rundsch 84 (3), 552–567. https://doi.org/10.1007/BF00284520.

Belousova, E.A., Kostitsyn, Y.A., Griffin, W.L., Begg, G.C., O'Reilly, S.Y., Pearson, N.J., 2010. The growth of the continental crust: constraints from zircon Hf-isotope data. Lithos 119 (3-4), 457–466. https://doi.org/10.1016/j.lithos.2010.07.024.

Berger, J., Féménias, O., Ohnenstetter, D., Bruguier, O., Plissart, G., Mercier, J.-C., Demaiffe, D., 2010. New occurrence of UHP eclogites in Limousin (French Massif Central): age, tectonic setting and fluid–rock interactions. Lithos 118 (3-4), 365–382. https://doi.org/10.1016/j.lithos.2010.05.013.

Blichert-Toft, J., Albarède, F., 1997. The Lu-Hf isotope geochemistry of chondrites and the evolution of the mantle-crust system. Earth Planet. Sc. Lett. 148 (1-2), 243–258. https://doi.org/10.1016/S0012-821X(97)00040-X.

Blichert-Toft, J., Chauvel, C., Albarède, F., 1997. Separation of Hf and Lu for high-precision isotope analysis of rock samples by magnetic sector-multiple collector ICP-MS. Contrib. Mineral. Petr. 127 (3), 248–260. https://doi.org/10.1007/s004100050278.

Boutelier, D., Chemenda, A., Burg, J.-P., 2003. Subduction versus accretion of intra-oceanic volcanic arcs: insight from thermo-mechanical analogue experiments. Earth Planet. Sci. Lett. 212 (1-2), 31–45. https://doi.org/10.1016/S0012-821X(03)00239-5.

Boynton, W.V., 1984. Cosmochemistry of the rare earth elements: meteorite studies. Developments in Geochemistry 2, 63–114. https://doi.org/10.1016/B978-0-444-42148-7.50008-3.

Bowes, D.R., Aftalion, M., 1991. U-Pb zircon isotopic evidence for early Ordovician and late Proterozoic units in the Marianske Lazne complex, Central European Hercynides. Neues Jahrbuch für Mineralogie Monatshefte 7, 315–326.

Casas, J.M., Murphy, J.B., 2018. Unfolding the arc: The use of pre-orogenic constraints to assess the evolution of the Variscan belt in Western Europe. Tectonophysics 736, 47–61. https://doi.org/10.1016/j.tecto.2018.04.012.

Cloos, M., 1993. Lithospheric buoyancy and collisional orogenesis: Subduction of oceanic plateaus, continental margins, island arcs, spreading ridges, and seamounts. Geol. Soc. Am. Bull. 105, 715–737. https://doi.org/10.1130/0016-7606(1993)105<0715:LBACOS>2.3.CO;2.

Collett, S., Štípská, P., Schulmann, K., Peřestý, V., Soldner, J., Anczkiewicz, R., Lexa, O., Kylander-Clark, A., 2018. Combined Lu-Hf and Sm-Nd geochronology of the Mariánské Lázně Complex: New constraints on the timing of eclogite-and granulite-facies metamorphism. Lithos 304, 74–94. https://doi.org/10.1016/j.lithos.2018.02.007.

Collett, S., Schulmann, K., Štípská, P., Míková, J., 2020. Chronological and geochemical constraints on the pre-variscan tectonic history of the Erzgebirge, Saxothuringian Zone. Gondwana Res. 79, 27–48. https://doi.org/10.1016/j.gr.2019.09.009.

Collett, S., Štípská, P., Schulmann, K., Míková, J., Kröner, A., 2021. Tectonic significance of the Variscan suture between Brunovistulia and the Bohemian Massif. J. Geol. Soc. London 178. doi: 10.1144/jgs2020-176.

Crowley, Q.G., Floyd, P.A., Štědrá, V., Winchester, J.A., Kachlík, V., Holland, J.G., 2002. The Mariánské-Lázně Complex, NW Bohemian Massif: development and destruction of an early Palaeozoic seaway. Geological Society, London, Special Publications 201 (1), 177–195.

Davidson, J., Turner, S., Plank, T., 2013. Dy/Dy*: variations arising from mantle sources and petrogenetic processes. J. Petrol. 54, 525–537. https://doi.org/10.1093/petrology/egs076.

Deiller, P., Štípská, P., Ulrich, M., Schulmann, K., Collett, S., Peřestý, V., Hacker, B., Kylander-Clark, A., Whitechurch, H., Lexa, O., Pelt, E., Míková, J., 2021. Eclogite subduction wedge intruded by arc-type magma: the earliest record of Variscan arc in the Bohemian Massif. Gondwana Res. 99, 220–246. https://doi.org/10.1016/j.gr.2021.07.005.

Deschamps, F., Godard, M., Guillot, S., Hattori, K., 2013. Geochemistry of subduction zone serpentinites: a review. Lithos 178, 96–127.

Dewey, J.F., Strachan, R.A., 2003. Changing Silurian-Devonian relative plate motion in the Caledonides: sinistral transpression to sinistral transtension. J. Geol. Soc. London 160 (2), 219–229. https://doi.org/10.1144/0016-764902-085.

Díez Fernández, R., Arenas, R., Sánchez Martínez, S., Novo-Fernández, I., Albert, R., 2020. Single subduction zone for the generation of Devonian ophiolites and high-P metamorphic belts of the Variscan Orogen (NW Iberia). Terra Nova 32 (4), 239–245. https://doi.org/10.1111/ter.12455.

Dörr, W., Zulauf, G., Fiala, J., Franke, W., Vejnar, Z., 2002. Neoproterozoic to Early Cambrian history of an active plate margin in the Teplá-Barrandian unit—a correlation of U-Pb isotopic-dilution-TIMS ages (Bohemia, Czech Republic). Tectonophysics 352 (1-2), 65–85. https://doi.org/10.1016/S0040-1951(02)00189-0.

Drost, K., Linnemann, U., McNaughton, N., Fatka, O., Kraft, P., Gehmlich, M., Tonk, C., Marek, J., 2004. New data on the Neoproterozoic-Cambrian geotectonic setting of the Teplá-Barrandian volcano-sedimentary successions: geochemistry, U-Pb zircon ages, and provenance (Bohemian Massif, Czech Republic). Int. J. Earth Sci. 93, 742–757. https://doi.org/10.1007/s00531-004-0416-5.

Drost, K., Gerdes, A., Jeffries, T., Linnemann, U., Storey, C., 2011. Provenance of Neoproterozoic and early Paleozoic siliciclastic rocks of the Teplá-Barrandian unit (Bohemian Massif): evidence from U-Pb detrital zircon ages. Gondwana Res. 19 (1), 213–231. https://doi.org/10.1016/j.gr.2010.05.003.

Edel, J.B., Schulmann, K., Lexa, O., Lardeaux, J.M., 2018. Late Palaeozoic palaeomagnetic and tectonic constraints for amalgamation of Pangea supercontinent in the European Variscan belt. Earth-Sci. Rev. 177, 589–612.

Faryad, S.W., 2012. High-pressure polymetamorphic garnet growth in eclogites from the Mariánské Lázně Complex (Bohemian Massif). Eur. J. Mineral. 24 (3), 483–497. https://doi.org/10.1127/0935-1221/2012/0024-2184.

Faryad, S.W., Jedlicka, R., Collett, S., 2013. Eclogite facies rocks of the Monotonous unit, clue to Variscan suture in the Moldanubian Zone (Bohemian Massif). Lithos 179, 353–363. https://doi.org/10.1016/j.lithos.2013.07.015.

Franke, W., 2000. The mid-European segment of the Variscides: tectonostratigraphic units, terrane boundaries and plate tectonic evolution. Geological Society, London, Special Publications 179 (1), 35–61.

Franke, W., Żelaźniewicz, A., 2002. Structure and evolution of the Bohemian Arc. Geological Society, London, Special Publications 201 (1), 279–293.

Franke, W., Cocks, L.R.M., Torsvik, T.H., 2017. The Palaeozoic Variscan oceans revisited. Gondwana Res. 48, 257–284. https://doi.org/10.1016/j.gr.2017.03.005.

Galbraith, R.F., Laslett, G.M., 1993. Statistical models for mixed fission track ages. Nuclear Tracks and Radiation Measurements 21 (4), 459–470. https://doi.org/10.1016/1359-0189(93)90185-C.

Gerya, T.V., Stöckhert, B., Perchuk, A.L., 2002. Exhumation of high-pressure metamorphic rocks in a subduction channel: a numerical simulation. Tectonics 21 (6), 6-1–6-19. https://doi.org/10.1029/2002TC001406.

Glen, R.A., Scheibner, E., VandenBerg, A.H.M., 1992. Paleozoic intraplate escape tectonics in Gondwanaland and major strike-slip duplication in the Lachlan orogen of southeastern Australia. Geology 20, 795–798. https://doi.org/10.1130/0091-7613(1992)020<0795:PIETIG>2.3.CO;2.

Godard, G., 2010. Two orogenic cycles recorded in eclogite-facies gneiss from the southern Armorican Massif (France). Eur. J. Mineral 21 (6), 1173–1190. https://doi.org/10.1127/0935-1221/2009/0021-1984.

Griffin, W.L., Pearson, N.J., Belousova, E., Jackson, S.E., van Achterbergh, E., O'Reilly, S.Y., Shee, S.R., 2000. The Hf isotope composition of cratonic mantle: LAM-MC-ICPMS analysis of zircon megacrysts in kimberlites. Geochim. Cosmochim. Acta 64 (1), 133–147. https://doi.org/10.1016/S0016-7037(99)00343-9.

Guillot, S., Ménot, R.-P., 2009. Paleozoic evolution of the external crystalline massifs of the Western Alps. C. R. Geosci. 341 (2-3), 253–265. https://doi.org/10.1016/j.crte.2008.11.010.

Hajná, J., Žák, J., Dörr, W., 2017. Time scales and mechanisms of growth of active margins of Gondwana: a model based on detrital zircon ages from the Neoproterozoic to Cambrian Blovice accretionary complex. Bohemian Massif. Gondwana Res. 42, 63–83. https://doi.org/10.1016/j.gr.2016.10.004.

Hajná, J., Žák, J., Dörr, W., Kachlík, V., Sláma, J., 2018. New constraints from detrital zircon ages on prolonged, multiphase transition from the Cadomian accretionary orogen to a passive margin of Gondwana. Precambrian Res. 317, 159–178. https://doi.org/10.1016/j.precamres.2018.08.013.

Hajná, J., Žák, J., Ackerman, L., Svojtka, M., Pašava, J., 2019. A giant late Precambrian chert-bearing olistostrome discovered in the Bohemian Massif: A record of Ocean Plate Stratigraphy (OPS) disrupted by mass-wasting along an outer trench slope. Gondwana Res. 74, 173–188. https://doi.org/10.1016/j.gr.2018.10.010.

Hall, P.S., Kincaid, C., 2001. Diapiric flow at subduction zones: a recipe for rapid transport. Science 292 (5526), 2472–2475.

Hanžl, P., Janoušek, V., Soejono, I., Buriánek, D., Svojtka, M., Hrdličková, K., Erban, V., Pin, C., 2019. The rise of the Brunovistulicum: age, geological, petrological and geochemical character of the Neoproterozoic magmatic rocks of the Central Basic Belt of the Brno Massif. Int. J. Earth Sci. 108 (4), 1165–1199. https://doi.org/10.1007/s00531-019-01700-2.

Hawkesworth, C.J., Gallagher, K., Hergt, J.M., McDermott, F., 1993. Mantle and slab contributions in arc magmas. Annu. Rev. Earth Planet. Sci. 21 (1), 175–204. https://doi.org/10.1146/annurev.ea.21.050193.001135.

Henderson, B.J., Collins, W.J., Murphy, J.B., Gutierrez-Alonso, G., Hand, M., 2016. Gondwanan basement terranes of the Variscan-Appalachian orogen: Baltican, Saharan and West African hafnium isotopic fingerprints in Avalonia, Iberia and the Armorican Terranes. Tectonophysics 681, 278–304. https://doi.org/10.1016/j.tecto.2015.11.020.

Hutton, D.H.W., 1987. Strike-slip terranes and a model for the evolution of the British and Irish Caledonides. Geol. Mag. 124 (5), 405–425. https://doi.org/10.1017/S0016756800017003.

Jagoutz, E., Palme, H., Baddenhausen, H., Blum, K., Cendales, M., Dreibus, G., Spettel, B., Lorenz, V., Wänke, H., 1979. The abundances of major, minor and trace elements in the Earth's mantle as derived from primitive ultramafic nodules. Lunar and Planetary Science Conference Proceedings 10, 2031–2050.

Janoušek, V., Farrow, C.M., Erban, V., 2006a. Interpretation of whole-rock geochemical data in igneous geochemistry: introducing Geochemical Data Toolkit (GCDkit). J. Petrol. 47, 1255–1259. https://doi.org/10.1093/petrology/egl013.

Janoušek, V., Gerdes, A., Vrána, S., Finger, F., Erban, V., Friedl, G., Braithwaite, C.J., 2006b. Low-pressure granulites of the Lišov Massif, Southern Bohemia: Viséan metamorphism of Late Devonian plutonic arc rocks. J. Petrol. 47, 705–744. https://doi.org/10.1093/petrology/egi091.

Janoušek, V., Jiang, Y., Buriánek, D., Schulmann, K., Hanžl, P., Soejono, I., Kröner, A., Altanbaatar, B., Erban, V., Lexa, O., Ganchuluun, T., Košler, J., 2018. Cambrian–ordovician magmatism of the Ikh-Mongol Arc system exemplified by the Khantaishir Magmatic Complex (Lake Zone, south–central Mongolia). Gondwana Res. 54, 122–149. https://doi.org/10.1016/j.gr.2017.10.003.

Jašarová, P., Racek, M., Jeřábek, P., Holub, F.V., 2016. Metamorphic reactions and textural changes in coronitic metagabbros from the Teplá Crystalline and Mariánské Lázně complexes, Bohemian Massif. J. Geosci-Czech 61, 193–219. https://doi.org/10.3190/jgeosci.216.

Jastrzębski, M., Budzyń, B., Żelaźniewicz, A., Konečný, P., Sláma, J., Kozub-Budzyń, G. A., Skrzypek, E., Jaźwa, A., 2021. Eo-Variscan metamorphism in the Bohemian Massif: Thermodynamic modelling and monazite geochronology of gneisses and granulites of the Góry Sowie Massif. SW Poland. J. Metamorph. Geol. 39 (6), 751–779. https://doi.org/10.1111/jmg.12589.

Jelínek, E., Štědrá, V., Cháb, J., 1997. The Mariánské Lázně Complex. Geological model of western Bohemia related to the KTB borehole in Germany. Czech. Geological Survey Prague, 61–70.

Kachlík, V., 1993. The evidence for Late Variscan nappe thrusting of the Mariánské Lázne Complex over the Saxothuringian terrane (West Bohemia). J. Geosci-Czech 38, 43–58.

Kastl, E., Tonika, J., 1984. The Mariánské Lázně metaophiolite complex (West Bohemia). Krystalinikum 17, 59–76.

Kelemen, P.B., Shimizu, N., Dunn, T., 1993. Relative depletion of niobium in some arc magmas and the continental crust: partitioning of K, Nb, La and Ce during melt/rock reaction in the upper mantle. Earth Planet Sci. Lett. 120 (3-4), 111–134. https://doi.org/10.1016/0012-821X(93)90234-Z.

Kemp, A.I.S., Hawkesworth, C.J., 2014. In: Treatise on Geochemistry. Elsevier, pp. 379–421. https://doi.org/10.1016/B978-0-08-095975-7.00312-0.

Koglin, N., Zeh, A., Franz, G., Schüssler, U., Glodny, J., Gerdes, A., Brätz, H., 2018. From Cadomian magmatic arc to Rheic ocean closure: the geochronological-geochemical record of nappe protoliths of the Münchberg Massif, NE Bavaria (Germany). Gondwana Res. 55, 135–152. https://doi.org/10.1016/j.gr.2017.11.001.

Konopásek, J., Anczkiewicz, R., Jeřábek, P., Corfu, F., Žáčková, E., 2019. Chronology of the Saxothuringian subduction in the West Sudetes (Bohemian Massif, Czech Republic and Poland). J. Geol. Soc. London 176 (3), 492–504. https://doi.org/10.1144/jgs2018-173.

Kotková, J., 2007. High-pressure granulites of the Bohemian Massif: recent advances and open questions. J. Geosci-Czech 52, 45–71. https://doi.org/10.3190/jgeosci.006.

Kotková, J., O'Brien, P.J., Ziemann, M.A., 2011. Diamond and coesite discovered in Saxony-type granulite: Solution to the Variscan garnet peridotite enigma. Geology 39, 667–670. doi: 10.1130/G31971.1.

Kroner, U., Romer, R.L., 2013. Two plates—many subduction zones: the Variscan orogeny reconsidered. Gondwana Res. 24 (1), 298–329. https://doi.org/10.1016/j.gr.2013.03.001.

Kryza, R., Fanning, C.M., 2007. Devonian deep-crustal metamorphism and exhumation in the Variscan Orogen: evidence from SHRIMP zircon ages from the HT-HP granulites and migmatites of the Góry Sowie (Polish Sudetes). Geodin. Acta 20 (3), 159–175. https://doi.org/10.3166/ga.20.159-175.

Kryza, R., Pin, C., 2010. The Central-Sudetic ophiolites (SW Poland): petrogenetic issues, geochronology and palaeotectonic implications. Gondwana Res. 17 (2-3), 292–305. https://doi.org/10.1016/j.gr.2009.11.001.

Kusbach, V., Janoušek, V., Hasalová, P., Schulmann, K., Fanning, C.M., Erban, V., Ulrich, S., 2015. Importance of crustal relamination in origin of the orogenic mantle peridotite–high-pressure granulite association: example from the Náměšť Granulite Massif (Bohemian Massif, Czech Republic). J. Geol. Soc. London 172 (4), 479–490. https://doi.org/10.1144/jgs2014-070.

Lancaster, P.J., Storey, C.D., Hawkesworth, C.J., Dhuime, B., 2011. Understanding the roles of crustal growth and preservation in the detrital zircon record. Earth Planet Sci Lett. 305 (3-4), 405–412. https://doi.org/10.1016/j.epsl.2011.03.022.

Lardeaux, J.M., Schulmann, K., Faure, M., Janoušek, V., Lexa, O., Skrzypek, E., Edel, J. B., Štípská, P., 2014. The Moldanubian Zone in the French Massif Central, Vosges/Schwarzwald and Bohemian Massif revisited: differences and similarities. Geological Society, London, Special Publications 405 (1), 7–44.
Lexa, O., Schulmann, K., Janoušek, V., Štípská, P., Guy, A., Racek, M., 2011. Heat sources and trigger mechanisms of exhumation of HP granulites in Variscan orogenic root. J. Metamorph. Geol. 29, 79–102. https://doi.org/10.1111/j.1525-1314.2010.00906.x.
Li, C., Arndt, N.T., Tang, Q., Ripley, E.M., 2015. Trace element indiscrimination diagrams. Lithos 232, 76–83. https://doi.org/10.1016/j.lithos.2015.06.022.
Linnemann, U., Romer, R.L., 2002. The Cadomian Orogeny in Saxo-Thuringia, Germany: geochemical and Nd–Sr–Pb isotopic characterization of marginal basins with constraints to geotectonic setting and provenance. Tectonophysics 352 (1-2), 33–64. https://doi.org/10.1016/S0040-1951(02)00188-9.
Li, X.H., Long, W.G., Li, Q.L., Liu, Y., Zheng, Y.F., Yang, Y.H., Chamberlain, K.R., Wan, D. F., Guo, C.H., Wang, X.C., Tao, H., 2010. Penglai zircon megacrysts: a potential new working reference material for microbeam determination of Hf–O isotopes and U–Pb age. Geostand.Geoanal. Res. 34, 117–134. https://doi.org/10.1111/j.1751-908X.2010.00036.x.
Liew, T.C., Hofmann, A.W., 1988. Precambrian crustal components, plutonic associations, plate environment of the Hercynian fold belt of central Europe: Indications from a Nd and Sr isotopic study. Contrib. Mineral. Petr. 98 (2), 129–138. https://doi.org/10.1007/BF00402106.
Linnemann, U., Gehmlich, M., Tichomirowa, M., Buschmann, B., Nasdala, L., Jonas, P., Lützner, H., Bombach, K., 2000. From Cadomian subduction to Early Palaeozoic rifting: the evolution of Saxo-Thuringia at the margin of Gondwana in the light of single zircon geochronology and basin development (Central European Variscides, Germany). Geological Society, London, Special Publications 179 (1), 131–153.
Linnemann, U., McNaughton, N.J., Romer, R.L., Gehmlich, M., Drost, K., Tonk, C., 2004. West African provenance for Saxo-Thuringia (Bohemian Massif): did Armorica ever leave pre-Pangean Gondwana?–U/Pb-SHRIMP zircon evidence and the Nd-isotopic record. Int. J. Earth Sci. 93 (5), 683–705. https://doi.org/10.1007/s00531-004-0413-8.
Maierová, P., Schulmann, K., Štípská, P., Gerya, T., Lexa, O., 2021. Trans-lithospheric diapirism explains the presence of ultra-high pressure rocks in the European Variscides. Commun. Earth Environ. 2 (56), 1–9. https://doi.org/10.1038/s43247-021-00122-w.
Martínez Catalán, J.R., Arenas, R., García, F.D., Cuadra, P.G., Gómez-Barreiro, J., Abati, J., Castiñeiras, P., Fernández-Suárez, J., Martínez, S.S., Andonaegui, P., Clavijo, E. G., 2007. Space and time in the tectonic evolution of the northwestern Iberian Massif: Implications for the Variscan belt. In: Hatcher, R.D., Carlson, M.P., McBride, J.H., Martínez Catalán, J.R. (Eds.), 4-D framework of continental crust. Geol. Soc. AM Mem. 200, 403–423. https://doi.org/10.1130/2007.1200(21).
Martínez Catalán, J.R., Collett, S., Schulmann, K., Aleksandrowski, P., Mazur, S., 2020. Correlation of allochthonous terranes and major tectonostratigraphic domains between NW Iberia and the Bohemian Massif, European Variscan belt. Int. J. Earth Sci. 109 (4), 1105–1131. https://doi.org/10.1007/s00531-019-01800-z.
Martínez Catalán, J.R., Schulmann, K., Ghienne, J.-F., 2021. The Mid-Variscan Allochthon: Keys from correlation, partial retrodeformation and plate-tectonic reconstruction to unlock the geometry of a non-cylindrical belt. Earth-Sci. Rev. 220, 103700. https://doi.org/10.1016/j.earscirev.2021.103700.
Mazur, S., Turniak, K., Bröcker, M., 2004. Neoproterozoic and Cambro-Ordovician magmatism in the Variscan Kłodzko metamorphic complex (West Sudetes, Poland): new insights from U/Pb zircon dating. Int. J. Earth Sci. 93, 758–772. https://doi.org/10.1007/s00531-004-0417-4.
Medaris, L.G., Beard, B.L., Johnson, C.M., Valley, J.W., Spicuzza, M.J., Jelínek, E., Mísâr, Z., 1995. Garnet pyroxenite and eclogite in the Bohemian Massif: geochemical evidence for Variscan recycling of subducted lithosphere. Geol. Rundsch 84 (3), 489–505. https://doi.org/10.1007/BF00284516.
Medaris, L.G., Beard, B.L., Jelínek, E., 2006. Mantle-derived, UHP garnet pyroxenite and eclogite in the Moldanubian Gföhl Nappe, Bohemian Massif: A geochemical review, new PT determinations, and tectonic interpretation. Int. Geol. Rev. 48 (9), 765–777. https://doi.org/10.2747/0020-6814.48.9.765.
Medaris, L.G., Jelínek, E., Faryad, S.W., Singer, B.S., 2011. Peridotite and metabasic rocks of the Mariánské Lázne Metaophiolite Complex/The Eclogitic Mariánské Lázne Complex: a Vestige of an Early Paleozoic Ocean. Geolines 23, 71–83.
Merdith, A.S., Williams, S.E., Collins, A.S., Tetley, M.G., Mulder, J.A., Blades, M.L., Young, A., Armistead, S.E., Cannon, J., Zahirovic, S., Müller, R.D., 2021. Extending full-plate tectonic models into deep time: Linking the Neoproterozoic and the Phanerozoic. Earth-Sci. Rev. 214, 103477. https://doi.org/10.1016/j.earscirev.2020.103477.
Murphy, J.B., Cousens, B.L., Braid, J.A., Strachan, R.A., Dostal, J., Keppie, J.D., Nance, R. D., 2011. Highly depleted oceanic lithosphere in the Rheic Ocean: implications for Paleozoic plate reconstructions. Lithos 123 (1-4), 165–175. https://doi.org/10.1016/j.lithos.2010.09.014.
Nahodilová, R., Štípská, P., Powell, R., Košler, J., Racek, M., 2014. High-Ti muscovite as a prograde relict in high pressure granulites with metamorphic Devonian zircon ages (Běstvina granulite body, Bohemian Massif): consequences for the relamination model of subducted crust. Gondwana Res. 25 (2), 630–648. https://doi.org/10.1016/j.gr.2012.08.021.
Nance, R.D., Murphy, J.B., 1994. Contrasting basement isotopic signatures and the palinspastic restoration of peripheral orogens: Example from the Neoproterozoic Avalonian-Cadomian belt. Geology 22 (7), 617. https://doi.org/10.1130/0091-7613(1994)022<0617:CBISAT>2.3.CO;2.
Nance, R.D., Murphy, J.B., Keppie, J.D., 2002. A Cordilleran model for the evolution of Avalonia. Tectonophysics 352 (1-2), 11–31.
Nance, R.D., Gutiérrez-Alonso, G., Keppie, J.D., Linnemann, U., Murphy, J.B., Quesada, C., Strachan, R.A., Woodcock, N.H., 2010. Evolution of the Rheic ocean. Gondwana Res. 17 (2-3), 194–222. https://doi.org/10.1016/j.gr.2009.08.001.
Nance, R.D., Gutiérrez-Alonso, G., Keppie, J.D., Linnemann, U., Murphy, J.B., Quesada, C., Strachan, R.A., Woodcock, N.H., 2012. A brief history of the Rheic Ocean. Geosci. Front. 3 (2), 125–135. https://doi.org/10.1016/j.gsf.2011.11.008.
O'Brien, P.J., 1997. Garnet zoning and reaction textures in overprinted eclogites, Bohemian Massif, European Variscides: a record of their thermal history during exhumation. Lithos 41 (1-3), 119–133. https://doi.org/10.1016/S0024-4937(97)82008-7.
Paquette, J.L., Ballèvre, M., Peucat, J.J., Cornen, G., 2017. From opening to subduction of an oceanic domain constrained by LA-ICP-MS U-Pb zircon dating (Variscan belt, Southern Armorican Massif, France). Lithos 294, 418–437. https://doi.org/10.1016/j.lithos.2017.10.005.
Paszkowski, M., Budzyń, B., Mazur, S., Sláma, J., Środoń, J., Millar, I.L., Shumlyanskyy, L., Kędzior, A., Liivamägi, S., 2021. Detrital zircon U-Pb and Hf constraints on provenance and timing of deposition of the Mesoproterozoic to Cambrian sedimentary cover of the East European Craton, part II: Ukraine. Precambrian Res. 362, 106282. https://doi.org/10.1016/j.precamres.2021.106282.
Paulick, H., Bach, W., Godard, M., De Hoog, J.C.M., Suhr, G., Harvey, J., 2006. Geochemistry of abyssal peridotites (Mid-Atlantic Ridge, 15 20′ N, ODP Leg 209): implications for fluid/rock interaction in slow spreading environments. Chem. Geol. 234 (3-4), 179–210. https://doi.org/10.1016/j.chemgeo.2006.04.011.
Pearce, J.A., 2008. Geochemical fingerprinting of oceanic basalts with applications to ophiolite classification and the search for Archean oceanic crust. Lithos 100 (1-4), 14–48. https://doi.org/10.1016/j.lithos.2007.06.016.
Peřestý, V., Lexa, O., Holder, R., Jeřábek, P., Racek, M., Štípská, P., Schulmann, K., Hacker, B., 2017. Metamorphic inheritance of Rheic passive margin evolution and its early-Variscan overprint in the Teplá-Barrandian Unit, Bohemian Massif. J. Metamorph. Geol. 35 (3), 327–355. https://doi.org/10.1111/jmg.12234.
Peřestý, V., Lexa, O., Jeřábek, P., 2020. Restoration of early-Variscan structures exposed along the Teplá shear zone in the Bohemian Massif: constraints from kinematic modelling. Int. J. Earth Sci. 109 (4), 1189–1211. https://doi.org/10.1007/s00531-019-01806-7.
Pertoldová, J., Verner, K., Vrána, S., Buriánek, D., Štědrá, V., Vondrovic, L., 2010. Comparison of lithology and tectonometamorphic evolution of units at the northern margin of the Moldanubian Zone: implications for geodynamic evolution in the northeastern part of the Bohemian Massif. J. Geosci-Czech 55, 299–319. https://doi.org/10.3190/jgeosci.083.
Pin, C., Kryza, R., Oberc-Dziedzic, T., Mazur, S., Turniak, K., Waldhausrová, J., 2007. In: The Evolution of the Rheic Ocean: From Avalonian-Cadomian Active Margin to Alleghenian-Variscan Collision. Geological Society of America. https://doi.org/10.1130/2007.2423(09).
Plank, T., Langmuir, C.H., 1998. The chemical composition of subducting sediment and its consequences for the crust and mantle. Chem. Geol. 145 (3-4), 325–394. https://doi.org/10.1016/S0009-2541(97)00150-2.
Pohlner, J.E., El Korh, A., Klemd, R., Grobéty, B., Pettke, T., Chiaradia, M., 2021. Trace element and oxygen isotope study of eclogites and associated rocks from the Münchberg Massif (Germany) with implications on the protolith origin and fluid-rock interactions. Chem. Geol. 579, 120352. https://doi.org/10.1016/j.chemgeo.2021.120352.
Ross, P.-S., Bédard, J.H., 2009. Magmatic affinity of modern and ancient subalkaline volcanic rocks determined from trace-element discriminant diagrams. Can. J. Earth Sci. 46 (11), 823–839. https://doi.org/10.1139/E09-054.
Sánchez Martínez, S., Arenas, R., Albert, R., Gerdes, A., Fernández-Suárez, J., 2021. Updated geochronology and isotope geochemistry of the Vila de Cruces Ophiolite: a case study of a peri-Gondwanan back-arc ophiolite. Geol. Soc. SP 503 (1), 497–530. https://doi.org/10.1144/SP503-2020-8.
Santolík, V., 2021. Petrogenesis and Evolution of the Davle Volcanic Complex. Charles University, Prague, p. 81 pp.. M.S. thesis.
Schmädicke, E., Mezger, K., Cosca, M.A., Okrusch, M., 1995. Variscan Sm-Nd and Ar-Ar ages of eclogite facies rocks from the Erzgebirge, Bohemian Massif. J. Metamorph. Geol. 13 (5), 537–552. https://doi.org/10.1111/j.1525-1314.1995.tb00241.x.
Schmädicke, E., Will, T.M., Ling, X., Li, X.H., Li, Q.L., 2018. Rare peak and ubiquitous post-peak zircon in eclogite: Constraints for the timing of UHP and HP metamorphism in Erzgebirge, Germany. Lithos 322, 250–267. https://doi.org/10.1016/j.lithos.2018.10.017.
Schulmann, K., Konopásek, J., Janoušek, V., Lexa, O., Lardeaux, J.-M., Edel, J.-B., Štípská, P., Ulrich, S., 2009. An Andean type Palaeozoic convergence in the Bohemian massif. C. R. Geosci. 341 (2-3), 266–286. https://doi.org/10.1016/j.crte.2008.12.006.
Schulmann, K., Lexa, O., Janoušek, V., Lardeaux, J.M., Edel, J.B., 2014. Anatomy of a diffuse cryptic suture zone: an example from the Bohemian Massif, European Variscides. Geology 42, 275–278. https://doi.org/10.1130/G35290.1.
Şengör, A.M.C., Natal'In, B.A., Burtman, V.S., 1993. Evolution of the Altaid tectonic collage and Palaeozoic crustal growth in Eurasia. Nature 364, 299–307. https://doi.org/10.1038/364299a0.
Söderlund, U., Patchett, P.J., Vervoort, J.D., Isachsen, C.E., 2004. The ^{176}Lu decay constant determined by Lu–Hf and U-Pb isotope systematics of Precambrian mafic intrusions. Earth Planet Sci. Lett. 219 (3-4), 311–324. https://doi.org/10.1016/S0012-821X(04)00012-3.

Spencer, C.J., Kirkland, C.L., Roberts, N.M.W., Evans, N.J., Liebmann, J., 2020. Strategies towards robust interpretations of in situ zircon Lu–Hf isotope analyses. Geosci. Front. 11 (3), 843–853. https://doi.org/10.1016/j.gsf.2019.09.004.

Stampfli, G.M., Hochard, C., Vérard, C., Wilhem, C., vonRaumer, J., 2013. The formation of Pangea. Tectonophysics 593, 1–19. https://doi.org/10.1016/j.tecto.2013.02.037.

Stephan, T., Kroner, U., Romer, R.L., 2019a. The pre-orogenic detrital zircon record of the Peri-Gondwanan crust. Geol. Mag. 156 (2), 281–307. https://doi.org/10.1017/S0016756818000031.

Stephan, T., Kroner, U., Romer, R.L., Rösel, D., 2019b. From a bipartite Gondwanan shelf to an arcuate Variscan belt: The early Paleozoic evolution of northern Peri-Gondwana. Earth-Sci. Rev. 192, 491–512. https://doi.org/10.1016/j.earscirev.2019.03.012.

Štípská, P., Powell, R., Hacker, B.R., Holder, R., Kylander-Clark, A.R.C., 2016. Uncoupled U/Pb and REE response in zircon during the transformation of eclogite to mafic and intermediate granulite (Blanský les, Bohemian Massif). J. Metamorph. Geol. 34, 551–572. https://doi.org/10.1111/jmg.12193.

Streckeisen, A.L., 1978. IUGS Subcommission on the Systematics of Igneous Rocks. Classification and Nomenclature of Volcanic Rocks, Lamprophyres, Carbonatites and Melilite Rocks. Recommendations and Suggestions. Neues Jahrbuch für Mineralogie, Abhandlungen 141, 1–14.

Sun, S.-s., McDonough, W.F., 1989. Chemical and isotopic systematics of oceanic basalts: implications for mantle composition and processes. Geological Society, London, Special Publications 42 (1), 313–345.

Tabaud, A.S., Štípská, P., Mazur, S., Schulmann, K., Míková, J., Wong, J., Sun, M., 2021. Evolution of a Cambro-Ordovician active margin in northern Gondwana: Geochemical and zircon geochronological evidence from the Góry Sowie metasedimentary rocks, Poland. Gondwana Res. 90, 1–26. https://doi.org/10.1016/j.gr.2020.10.011.

Tasáryová, Z., Janoušek, V., Frýda, J., 2018. Failed Silurian continental rifting at the NW margin of Gondwana: evidence from basaltic volcanism of the Prague Basin (Teplá–Barrandian Unit, Bohemian Massif). Int. J. Earth Sci. 107 (4), 1231–1266. https://doi.org/10.1007/s00531-017-1530-5.

Taylor, S.R., McLennan, S.M., 1995. The geochemical evolution of the continental crust. Rev. Geophys. 33, 241–265. https://doi.org/10.1029/95RG00262.

Thirlwall, M.F., Walder, A.J., 1995. In situ hafnium isotope ratio analysis of zircon by inductively coupled plasma multiple collector mass spectrometry. Chem. Geol. 122 (1-4), 241–247. https://doi.org/10.1016/0009-2541(95)00003-5.

Tiepolo, M., Bottazzi, P., Foley, S.F., Oberti, R., Vannucci, R., Zanetti, A., 2001. Fractionation of Nb and Ta from Zr and Hf at mantle depths: the role of titanian pargasite and kaersutite. J. Petrol. 42, 221–232. https://doi.org/10.1093/petrology/42.1.221.

Timmermann, H., Štědrá, V., Gerdes, A., Noble, S.R., Parrish, R.R., Dörr, W., 2004. The problem of dating high-pressure metamorphism: a U-Pb isotope and geochemical study on eclogites and related rocks of the Mariánské Lázně Complex, Czech Republic. J. Petrol. 45, 1311–1338. https://doi.org/10.1093/petrology/egh020.

Timmermann, H., Dörr, W., Krenn, E., Finger, F., Zulauf, G., 2006. Conventional and in situ geochronology of the Teplá Crystalline unit, Bohemian Massif: implications for the processes involving monazite formation. Int. J. Earth Sci. 95 (4), 629–647. https://doi.org/10.1007/s00531-005-0060-8.

Vermeesch, P., 2018. IsoplotR: A free and open toolbox for geochronology. Geosci. Front. 9 (5), 1479–1493. https://doi.org/10.1016/j.gsf.2018.04.001.

Warren, C.J., Beaumont, C., Jamieson, R.A., 2008. Modelling tectonic styles and ultra-high pressure (UHP) rock exhumation during the transition from oceanic subduction to continental collision. Earth Planet Sci. Lett. 267 (1-2), 129–145. https://doi.org/10.1016/j.epsl.2007.11.025.

Winchester, J.A., Floyd, P.A., 1977. Geochemical discrimination of different magma series and their differentiation products using immobile elements. Chem. Geol. 20, 325–343. https://doi.org/10.1016/0009-2541(77)90057-2.

Yamato, P., Agard, P., Burov, E., Le Pourhiet, L., Jolivet, L., Tiberi, C., 2007. Burial and exhumation in a subduction wedge: mutual constraints from thermomechanical modeling and natural P-T-t data (Schistes Lustrés, western Alps). J. Geophys. Res.-Sol. Ea. 112 (B7), B07410. https://doi.org/10.1029/2006JB004441.

Yin, A.n., Manning, C.E., Lovera, O., Menold, C.A., Chen, X., Gehrels, G.E., 2007. Early Paleozoic tectonic and thermomechanical evolution of ultrahigh-pressure (UHP) metamorphic rocks in the northern Tibetan Plateau, northwest China. Int. Geol. Rev. 49 (8), 681–716. https://doi.org/10.2747/0020-6814.49.8.681.

Žák, J., Kratinová, Z., Trubač, J., Janoušek, V., Sláma, J., Mrlina, J., 2011. Structure, emplacement, and tectonic setting of Late Devonian granitoid plutons in the Teplá-Barrandian unit, Bohemian Massif. Int. J. Earth Sci. 100 (7), 1477–1495. https://doi.org/10.1007/s00531-010-0565-7.

Žák, J., Svojtka, M., Hajná, J., Ackerman, L., 2020. Detrital zircon geochronology and processes in accretionary wedges. Earth-Sci. Rev. 207, 103214. https://doi.org/10.1016/j.earscirev.2020.103214.

Závada, P., Štípská, P., Hasalová, P., Racek, M., Jeřábek, P., Schulmann, K., Kylander-Clark, A., Holder, R., 2021. Monazite geochronology in melt-percolated UHP meta-granitoids: An example from the Erzgebirge continental subduction wedge, Bohemian Massif. Chem. Geol. 559, 119919. https://doi.org/10.1016/j.chemgeo.2020.119919.

Zeh, A., Will, T.M., 2010. The mid-German crystalline zone. In: Linemmann, U., Kroner, U., Romer, R.L. (Eds.), Pre-Mesozoic Geology of Saxo-Thuringia—From the Cadomian Active Margin to the Variscan Orogen. Schweizerbart, Stuttgart, pp. 195–220.

Zhang, L.e., Ren, Z.-Y., Nichols, A.R.L., Zhang, Y.-H., Zhang, Y., Qian, S.-P., Liu, J.-Q., 2014. Lead isotope analysis of melt inclusions by LA-MC-ICP-MS. J. Anal. Atom. Spec. 29 (8), 1393–1405. https://doi.org/10.1039/C4JA00088A.

Štědrá, V., 2001. Tectonometamorphic evolution of the Marianske lazne Complex, Western Bohemia, based on the study of metabasic rocks. (Ph.D. thesis). Charles University: Prague, 164